NPS-61Md73101A

NAVAL POSTGRADUATE SCHOOL
Monterey, California

31 October 1973 NPS-61Md73101A

SOUND SPEED DISPERSION AND FLUCTUATIONS
IN THE UPPER OCEAN: PROJECT BASS

H. Medwin
Dept of Physics & Chemistry

NAVAL POSTGRADUATE SCHOOL
Monterey, California

Rear Admiral M. B. Freeman
Superintendent

M. U. Clauser
Provost

TITLE: Sound Speed Dispersion and Fluctuations in the Upper Ocean: Project BASS

AUTHOR: H. Medwin

ABSTRACT:

Simultaneous measurements of ocean microstructure and sound phase shift from a stable platform in BASS STRAIT, AUSTRALIA, have provided new relations between the statistics of the medium and the statistics of the local sound phase speed near the sea surface in the open ocean. Because of dispersion due to ambient bubbles, average phase speeds in the frequency range 15 to 100 kHz differ as much as 2.5m/sec from the accepted 3MHz "precision" velocimeter values down to depths of 7.6m in the presence of wind speeds of 25-30 knots. These differential speeds imply average bubble volume fractions of the order of 10^{-7} with standard deviations approximately one-fifth of the mean value. The differential sound speed is now shown to increase approximately proportional to the wind speed. The third power decrease of differential speed with increasing depth is roughly verified. Under these experimental conditions the predominant cause of the local phase fluctuations at 24.4 and 95.6 kHz is shown to be bubble activity rather than temperature fluctuations. At 24.4 kHz the activity is the random change of number of bubbles. At a frequency such as 95.6 kHz, where there is a large resonant bubble population, the predominant part of the frequency spectrum of the sound phase modulation is shown to be caused by changing bubble radius due to the fluctuating ocean surface wave height. The sound phase spectrum mimics the wind wave spectrum given by Pierson and Moskovitz to two octaves beyond the frequency of the peak energy, at which point the surface pressure effect has dropped low enough for temperature fluctuations to take over. A theory is presented for prediction of these microstructural sound phase fluctuations from a knowledge of the surface wave height spectrum.

This task was supported by Code 302, Naval Ship Systems Command, and the Royal Australian Naval Research Laboratory.

TABLE OF CONTENTS

I. INTRODUCTION

The objective of this research was to study the relations between acoustic phase shifts and the fluctuating parameters of the near surface ocean. Time series data of the acoustic phase were used to calculate the dependence of the standard deviation and the mean value of the sound speed on frequency, range and depth. Simultaneous measurements were made of the fluctuating temperature, two components of particle velocity and standard acoustic velocimeter output.

The research was conducted using the BHP/ESSO Ocean Drilling Platform "Kingfish A", Lat. 38°, 39.5' S, Long. 148°, 08.7' E, Bass Strait, southeast of Victoria, Australia, as a test platform. The platform is about 50 miles from shore and stands in water approximately 250 feet deep. Data were collected during two visits to the tower: BASS I (20-25 November 1972) and BASS II (12-18 February 1973).

This report is being issued jointly with the Royal Australian Naval Research Laboratory, Garden Island, 2000, Australia.

II. BACKGROUND

Following the early work of Minnaert (1933) both Germany[1] and the United States and its allies[2] conducted extensive theoretical and applied research during and following World War II to evaluate the importance of ocean bubbles in the propagation of underwater sound. By the end of the 1950s, the physical understanding of bubble action in the presence of a sound wave was secure[3] and in the 1960s research spread to many adjacent areas including chemical engineering, nuclear physics, and oceanography and even meteorology[4].

The question of whether there are bubbles in the ocean, without the intrusion of man-made vehicles, has remained controversial. Those who tend to doubt the existence of ambient bubbles in the sea quote the laboratory experiments of Liebermann[5], who demonstrated the rapid loss of bubbles due to buoyancy and diffusion. On the other side of the controversy, there have been measurements[6] showing that bubbles are produced by wind waves and decaying matter on the ocean floor[7]. Marine biologists have no doubts about the continual generation of bubbles in the sea by photosynthesis, and marine life. The root question, of course, is whether those bubbles that are produced by physical and biological activities in the sea are so numerous that in-situ measurements will always detect ambient bubbles and, more directly for the underwater acoustician, the question is whether ambient bubbles are numerous enough to influence sound propagation.

The Ocean Physics Laboratory at the Naval Postgraduate School conducted a student research program to determine the excess attenuation and scatter from near surface bubbles from 1963 through 1965. This early work[8,9] was summarized in a recent publication[10] which showed the results of photographing bubbles and of in-situ acoustical attenuation and scattering measurements at the Naval Underwater Center's oceanographic tower in San Diego, California, and in Monterey Bay. Measurements were made from the surface to depths of 45 ft. Bubble volume fractions of the order of 10^{-10} or greater in a one micron radius increment were typical. The dominant sound frequencies that would be affected were in the measurement range, above about 25 kHz, but theory indicates that significant dispersion of sound speed should also be found for frequencies lower than the measured ones.

The Ocean Physics Laboratory set out to measure, directly, the change of

sound speed with sound frequency, implied by the previous determinations of attenuation and scatter near the sea surface. Results of measurements[11] from the NUC tower at San Diego in October 1971, showed unmistakable evidence of dispersion of the speed of sound. Deviations of the propagation speed with frequency were of the order of meters/second greater or less than the "theoretical" speed calculated from the traditional parameters of temperature, salinity and depth. The standard deviations of the speed measurements were much less than the deviations of the measured speed from the theoretical speed. Bubble populations were identifiable at depths 4.3m and 9.3m, which, when converted to surface values on the basis of constant mass and isothermal transport, represent 62 micron (52 kHz) bubbles and 100 micron (32 kHz) bubbles. The power spectral density of the time-varying sound speed peaked at frequencies less than 0.5 Hz, suggesting that bubbles were entrained at orbital frequencies associated with the ocean surface wave system.

During 1972, our group mounted three simultaneous attacks in order to understand better the dynamics of bubble populations in the upper ocean. Transport analysis[12] of the effects of buoyancy, gas diffusion and vertical velocities of the medium showed that bubbles which originate at the surface would require large downward convective velocities to persist at depth; large bubbles which originate in the sediment rise to the surface with little evidence of gas diffusion; an exponentially decaying volume source (maximum at the surface) would show ambient distributions that mimic the source function, if the bubbles are large, and would show much greater variation from the source distribution as a result of gas diffusion, if the bubbles are small.

A study[13] of the statistics of fluctuations of sound speed due to bubble populations showed that the maximum fluctuations due to changes in number of

bubbles would occur at frequencies displaced from the resonant frequency by amounts $f_R/(1 \pm \delta)^{\frac{1}{2}}$. The standard deviation would be greater at the lower frequency than at the upper one. f_R = resonant frequency, δ = damping constant.

An experimental study[14] of sound speed at the Naval Underwater Center oceanographic tower in June 1972, covered the extended frequency range 15 to 150 kHz in increments of approximately 3.5 kHz at a depth of 3.1 ± 0.3 meters. Both average speed and standard deviation of speed were determined at each frequency. An analysis[13] of the experimental data showed that the statistical theory predictions of frequencies of maximum fluctuation of sound speed agreed with the experimental measurements for at least four identifiable bubble populations of surface equivalent radii 54, 76, 105 and 200 microns, resonant at surface equivalent frequencies of 60, 43, 31, 16 kHz, respectively. Correlations between sound phase and ocean surface height revealed that there are strong fluctuations in the sound speed, in phase with the surface height fluctuations, at sound frequencies that correspond to the resonant frequencies of the peak bubble concentrations.

The purpose of the BASS experiments was to repeat, in the waters of the South Pacific, some of the San Diego experiments and to look for the statistics of the correlations with speed fluctuations and its temperature microstructure and medium particle velocity as a function of depth and sound frequency.

III. THEORY

A. Phase Speed in a Bubbly Medium

1. Bubbles of One Size Only

The presence of bubbles in a water medium affects the speed of sound because of the changed compressibility. Although there is also a potential

effect on the speed caused by the reduced density of the medium, we are interested only in the ocean medium, for which the density change can readily be shown to be negligible for realistic environments.

The dependence of the speed on the compressibility and density is given by

$$c^2 = \frac{1}{\rho K} \tag{1}$$

The compressibility of the bubbly medium, K, is made up of a part due to the water, K_o, and the part involving the change in volume of the bubbles, K_1,

$$K = K_o + K_1$$

The compressibility of the bubble-free water is most simply expressed in terms of the usual value of the speed of sound through water, c_o, and the density, ρ_o,

$$K_o = \frac{1}{\rho_o c_o^2} \tag{2}$$

The speed through the bubble-free water can be obtained from a simplified form of Wilson's equation

$$c_o = 1449. + 4.6t - 0.055t^2 + 0.017d \tag{2a}$$

where t = temperature [°C], d = depth [meters], and salinity is assumed 35 ppt.

The more sensitive compressibility, due to the bubbles, is given by

$$\underset{\sim}{K}_1 = \frac{\underset{\sim}{\Delta V}}{P_p} = \frac{N\underset{\sim}{\Delta v}}{P_p} = \frac{NS\underset{\sim}{\xi}_o}{P_p} = \frac{NS^2}{m\omega^2\left[\left(-1 + \frac{\omega_R^2}{\omega^2}\right) + j\,\frac{R}{\omega m}\right]} \tag{3}$$

where N = number of bubbles of radius, a

Δv = change in volume for each bubble in incident field, P_p

$S = 4\pi a^2$ = surface area of each bubble

and $\underset{\sim}{\xi}_o$ = complex magnitude of radial displacement of bubble surface.

The compressibility, $\underset{\sim}{K}$, is written in complex notation because of its dependence on the radial displacement, $\underset{\sim}{\xi}_o$, which is itself complex. Simplification occurs if we now insert $\underset{\sim}{\xi}_o$ and also define

$$Z = f_R/f = \omega_R/\omega \tag{4}$$

and

$$\delta = R/\omega m \tag{5}$$

Then,

$$\underset{\sim}{K}_1 = \frac{N4\pi a\,[Z^2 - 1 - j\delta]}{\rho_o \omega^2\,[(Z^2 - 1)^2 + \delta^2]} \tag{6}$$

and

$$\underset{\sim}{K} = K_o + \underset{\sim}{K}_1 = \frac{1}{\rho_o c_o^{\,2}} + \frac{4\pi a N[Z^2 - 1 - j\delta]}{\rho_o \omega^2\,[(Z^2 - 1)^2 + \delta^2]} \tag{7}$$

The expression for the speed of sound in the bubbly medium is now

$$\underset{\sim}{c} = \left(\frac{1}{\rho_o \underset{\sim}{K}}\right)^{\frac{1}{2}} = \frac{c_o}{\left[1 + \frac{4\pi a N c_o^{\,2}}{\omega^2}\left(\frac{Z^2 - 1 - j\delta}{(Z^2 - 1)^2 + \delta^2}\right)\right]^{\frac{1}{2}}} \tag{8}$$

and the real part of $\underset{\sim}{c}$ is

$$\mathrm{Re}\{\underset{\sim}{c}\} = c_o\left[1 - \frac{2\pi a N c_o^{\,2}}{\omega^2}\,\frac{(Z^2 - 1)}{(Z^2 - 1)^2 + \delta^2}\right] \tag{9}$$

Before interpreting our result, it is useful to put the bubble measurement in terms of the fraction of gas in bubble form, U(a), defined for bubbles of radius, a, by

$$U(a) = \left[N(a)\right]\left[\frac{4}{3}\pi a^3\right]$$

Then,

$$\mathrm{Re}\{\underset{\sim}{c}\} = c_o\left[1 - \frac{3UZ^2}{2a^2 k_R^{\,2}}\,\frac{Z^2 - 1}{\left(Z^2 - 1\right)^2 + \delta^2}\right] \tag{10}$$

It is of interest to look at the special cases for frequencies, (a) much less than the resonant frequency of the bubbles, (b) much greater than the resonant frequency, and (c) close to the resonant frequency. For simplicity, the reduction is carried out for standard, sea level conditions.

(a) $f \ll f_R$, $Z \gg 1$

$$c = c_o \left[1 - \frac{3U}{2a^2 k_R^2} \right] \tag{11}$$

then, since at sea level $ak_R = 1.36 \times 10^{-2}$, the speed reduces to $c = c_o[1 - 8.1 \times 10^3 \, U(a)]$ and the value is found to be less than c_o, independent of the particular frequency, f, and dependent only on the fractional volume of gas to water, U(a).

(b) $f \gg f_R$, $Z \ll 1$

At sea level, the speed has the value

$$c = c_o \left[1 + 8.1 \times 10^3 \, U(a) \, \frac{Z^2}{1 + \delta^2} \right] \tag{12}$$

which is greater than the bubble-free value c_o, dependent on the particular frequency and damping constant, reaching the value c_o only as the frequency approaches infinity.

(c) $f \approx f_R$, $Z \approx 1$

The speed in the bubbly water is c_o at the resonant frequency. It rises rapidly to a peak at frequencies slightly greater than f_R, and drops rapidly to a minimum at frequencies slightly less than f_R.

The detailed behavior of the speed, near the resonant frequency, is

shown in Fig. 1, which has been drawn for two cases of different numbers of bubbles. The change in speed has been presented in terms of the shift in speed $\delta c = (c - c_o)$ at frequency ratio f/f_R. It is interesting to observe that the maxima and minima of the resonant swings occur at frequencies given approximately by $f = f_R(1 \pm \delta_R/2)$. That is, for $\delta_R = 0.10$, the peak and trough of the resonance are $\delta_R/2 \sim 5\%$ above and below the resonant frequency. The magnitudes of the speed at these points are above and below the speed in bubble-free water by an amount approximately $\frac{1}{2\delta_R}$ times the value at the zero frequency limit given by equation (11).

Study of equation (10), which led us to Figure 1, shows that the speed of sound is significantly altered even at frequencies far from the resonance frequency. For example, for the case of $\delta_R = 0.1$, the speed at $f/f_R = 2$ is still approximately 0.33 (8.1×10^3 Uc_o) above the bubble-free value which exists as f approaches infinity. And at $f/f_R = 0.5$, the lowered value of the speed is 0.33 (8.1×10^3 Uc_o) less than the asymptotic value achieved as the frequency approaches zero.

2. Bubbles of many Sizes.

The generalization of our results to a cluster of bubbles of various radii is accomplished by including additional terms in equation (7). It is easy to handle the situation for a broad range of radii, such as exists in the ocean, by replacing N(a) by n(a)da = number of bubbles per unit volume with radius between a and a + da. Similarly, U(a) is replaced by u(a)da to represent the volume fraction of gas in bubble form to liquid. Then, instead of $\underset{\sim}{K}_{ij}$, as in equation (7), we write

$$\underset{\sim}{K}_{ij} = \int_{a_i} \frac{4\pi a_i n_i(a_i) da_i}{\rho_o \omega^2} \frac{\left[Z_i^2 - 1 - j\delta_{iR} \right]}{\left[\left(Z_i^2 - 1 \right)^2 + \delta_{iR}^2 \right]} \qquad (13)$$

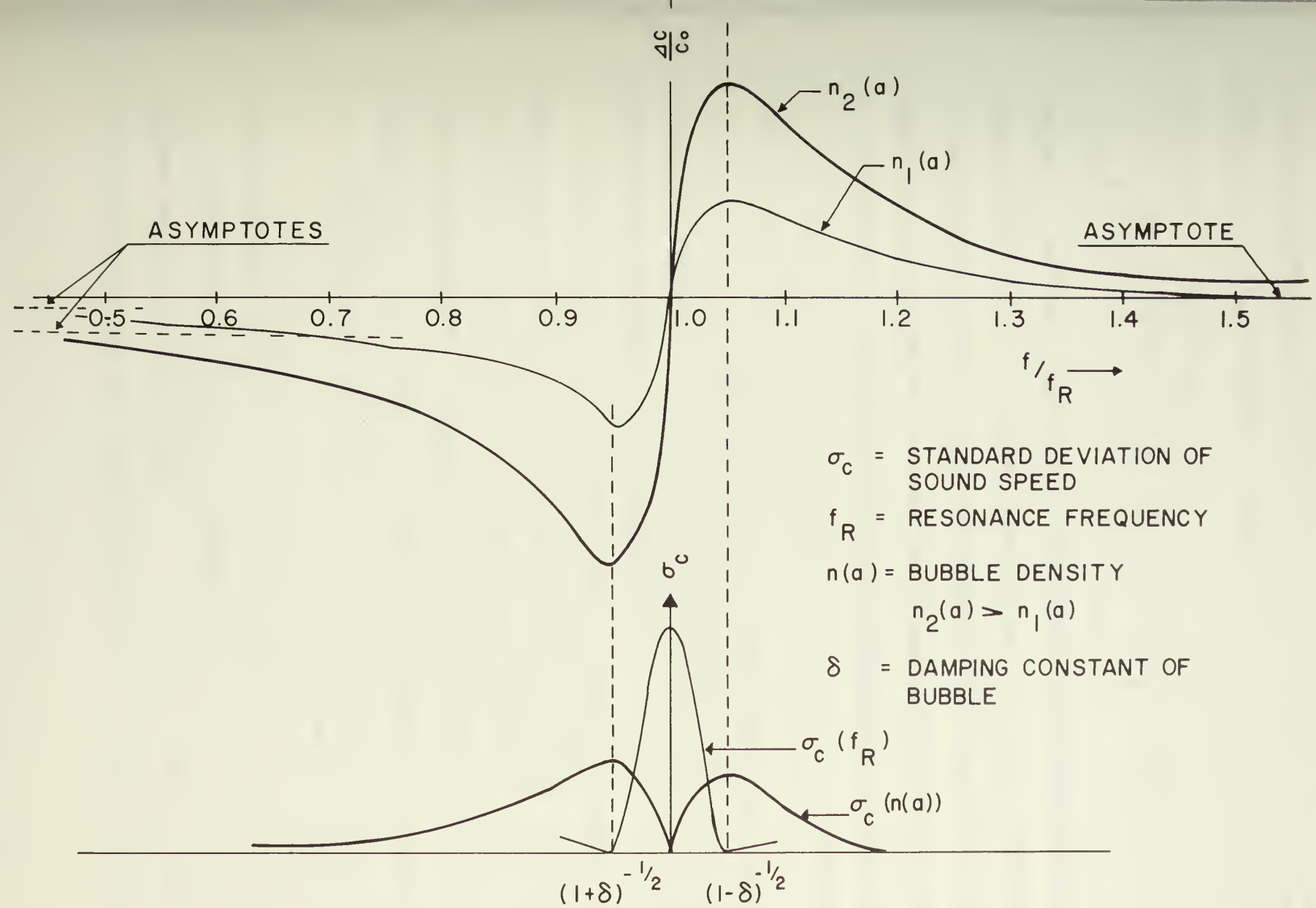

Fig 1. The dispersion of sound speed in a bubbly region of water. The abscissa is the relative frequency, f/f_R, where f_R is the bubble resonance frequency. The ordinate is the relative change in sound speed, compared to the bubble-free value. The lower curve shows the standard deviation of the phase speed as a result of change of bubble resonant frequency, $\sigma_c(f_R)$, and change of number of bubbles, $\sigma_c(n(a))$.

Because all contributions to the compressibility are very small quantities, they add linearly and the speed of sound in the bubble region can be written

$$\mathrm{Re}\{\underset{\sim}{c}\} = c_o \left[1 - \frac{3}{2} \int_{a_i} \frac{u(a_i) Z_i^{\,2} \left(Z_i^{\,2} - 1 \right) da_i}{a_i^{\,2} k_{iR}^{\,2} \left[\left(Z_i^{\,2} - 1 \right)^2 + \delta_{iR}^{\,2} \right]} \right] \qquad (14)$$

The effect of a mixture of bubble sizes around a peak population at resonance frequency, f_R, is to smear the dispersion curve for the speed so that, although the magnitudes of the deviation from the bubble free value are increased, the frequency range between the peak and the trough is also increased beyond the value that we calculated in Section A for the single bubble size.

B. Statistics of Phase Speed in a Fluctuating Medium

The near-surface region of the ocean is a medium that shows spatial and temporal fluctuations of the temperature, salinity, pressure, and three components of particle velocity. Sound propagation takes place in such a medium only at the cost of sound phase and amplitude fluctuations along the acoustic path. The phenomena have been studied theoretically under rather major simplifying assumptions[16]. Recent experimental research has extended these studies to the near-surface region of the ocean[17], in order to search for the real world correlations between the sound fluctuations and the fluctuations of the medium.

Fluctuations in the speed of sound, measured[11] near the ocean surface, have been shown to have a Gaussian probability density function except in the regions of large differential speed of sound, where the PDF was double-peaked. The temporal correlation time for phase was about the same as for

the oceanographic variables. The power spectral density of the time-varying phase showed evidence of bubbles entrained at orbital frequencies associated with the surface wave system.

Work at the Naval Postgraduate School[17] has also revealed that orbital motion due to surface wave action shifts inhomogeneities of temperature, salinity, and bubbles, and causes phase changes of sound propagated near the surface. Phase modulation envelopes were found to have smaller correlation times and spatial correlation lengths in the mixed layer than in the thermocline. Correlation times were greater for propagation in the vertical than in the horizontal directions in the thermocline. Anisotropy in the thermocline was also indicated by the variance of phase fluctuation being greater for horizontal than vertical propagation.

Cross-correlations between ocean surface height and sound phase[14] have been shown to be very large at the sound frequencies where dispersion of the speed indicated large populations of bubbles.

For the purpose of this report it will not be necessary to look at all of the details of the mechanisms for sound speed fluctuations. The problem can be discussed adequately if we simply point out that the variance of the speed fluctuation can, in principle, be due to any of the medium descriptors mentioned in the first paragraph of this section. However, realistically, fluctuations in salinity and density can readily be shown (from eq (2a) to be negligible. Furthermore, it is possible to subtract out the effects of motion of the medium either by a double path, as in the case of commercial velocimeters, or by subtracting out the effect of the motion indicated by a velocity flowmeter, as we have done. It is the latter technique that has been used in this experiment. This leaves fluctuating bubbles and temperature

as the major sources of sound speed variation.

It is possible to calculate the variance of the speed fluctuations due to temperature, simply and effectively enough for the purposes of this study, by linearizing equation (2a) and rewriting it as

$$c_o = c_{ref} + bt \tag{15}$$

For water of temperature 19° C, the linearization parameters are:

$$c_{ref} = 1471.25 \text{ m/sec}$$
$$b = 2.66 \ (^\circ C)^{-1}$$

The variable effect of bubbles is due to (a) changes of total gas in bubble form, U, or (b) changes of the bubble distribution with radius, or (c) perturbation of the resonant frequency of a predominant population at the frequency of the study. The source of fluctuation (a) has been considered carefully[13] and it has been shown that the maxima occur at frequencies given by $f = f_R(1 \pm \delta_R/2)$ for resonant frequency, f_R, with damping constant, δ_R.

There is little information about preferential sizes of bubbles for specific bubble-making processes. However, there is no reason to assume that the average distribution of bubble numbers with radius at a given depth and time of day will change, except by rather small amounts during a propagation experiment. We will assume that fluctuation source (b) is negligible.

Finally, (c) perturbation of the resonant frequency can have a profound effect on the variation of the speed of sound and it appears that the change of water pressure (due to surface wave action) at the level of the experiment can modulate the resonant frequency as given by the equation

$$f_R = \frac{1}{2\pi a} \sqrt{\frac{3\gamma P_o}{\rho_o}} \tag{16}$$

where P_o = ambient pressure

ρ_o = ambient density

and thereby cause the speed of sound to move up and down the steep part of the speed curve, as shown in Figure 1. If this action occurs during propagation of a frequency that corresponds to a major bubble population, a very large variance of sound phase can occur.

The effect of bubbles in changing the speed of sound can also be linearized if we restrict our interest to one frequency at a time. Then, in a bubbly medium

$$c = c_o \left[1 + \delta c(U,f)\right] \tag{17}$$

where $\delta c(U,f)$ is the increment in speed due to bubbles. Combining equations (15) and (17), since both bT and $\delta c(U,f)$ are very small compared to unity, the expression for the speed of sound can be written

$$c \approx c_{ref} + bT + \delta c \tag{18}$$

from which the variance of the speed is

$$\text{Var}\{c\} = b^2 \text{ Var}\{T\} + \text{Var}\{\delta c\} \tag{19}$$

Experimental values of the variance of δc can be used in two ways:

(a) At very low frequencies, equation (11) leads to

$$\text{Var}\{\delta c\} = \frac{9c_o^2}{4a^2k_R^2} \text{ Var}\{U\} \quad , \quad f \ll f_R \ , \tag{20}$$

so that the variance of changes of total fraction of bubble volume, Var {U}, can be calculated.

(b) At frequencies that show 100% cross-correlation of sound phase with the surface wave height, it can be assumed that the high

correlation is completely due to resonant frequency fluctuation caused by pressure and radius perturbations defined by equation (16) near $Z = f_R/f = 1$. A change of f_R at constant f can be understood by considering the speed change shown in Figure 1. At $f/f_R = 1$, there is a maximum rate of change of c with change of the ratio. For bubbles beyond the peak and trough of the dispersion curve, the effect of change of f/f_R is very much less, and goes in the opposite direction. A positive 100% cross-correlation with wave height would suggest that phase changes near Z = 1 override changes in the opposite direction in the outer regions of the dispersion curves of the much large and much smaller bubbles.

We consider the region near Z = 1 by defining

$$Z = f_R/f = 1 + \Delta \qquad \text{where } \Delta \ll 1 \qquad (21)$$

$$\Delta = \frac{\sqrt{3\gamma P_o/\rho}}{2\pi a f} - 1 \qquad \text{for } Z \approx 1 \qquad (22)$$

For the slow changes accompanying the ocean wave system we can assume the isothermal relation

$$da/dP = -\frac{a}{3P} \quad .$$

Differentiation of the above equation then gives the rate of change

$$\frac{d\Delta}{dP} = \frac{5}{6P}(1 + \Delta) \qquad (23)$$

Integration between limits

$$\Delta_1 = Z_1 - 1 = 0 \quad \text{at } P_1 = P_s\left(1 + \frac{d,m}{10m}\right)$$

and $$\Delta_2 = \Delta \qquad \text{at } P_2 = P_s\left(1 + \frac{d,m}{10m} + \frac{h,m}{10m}\right)$$

yields

$$\Delta - \frac{\Delta^2}{2} = \frac{5}{6} \ell n \left[1 + \frac{h,m/10m}{1 + \frac{d,m}{10m}} \right] \tag{24}$$

where P_s = surface ambient pressure = 1 atmosphere

d,m = experiment depth in meters

h,m = wave height in meters

The expansion for small increments is used

$$\ell n(1 + x) = x - \frac{1}{2} x^2 + - - -$$

where $x = \dfrac{h,m/10m}{1 + \dfrac{d,m}{10m}}$

to give

$$\Delta \approx \frac{5}{6} \left[\frac{h,m/10m}{1 + \frac{d,m}{10m}} \right] \tag{25}$$

Using the approximation $Z = 1 + \Delta$ and taking the variance of both sides of equation (10), we get

$$\text{Var } \{\delta c(\Delta)\} = \text{Var} \left\{ c_o \left[1 - \frac{U\rho {c_o}^2 \Delta}{\gamma P_o (4\Delta^2 + \delta^2} \right] \right\} \text{ to order } \Delta^2 \ll 1. \tag{26}$$

If we assume that $4\Delta^2 \ll \delta^2$ (e.g., much less than a 5% variation in f_R/f for a 60 micron bubble) and use equation (24), we get

$$\text{Var } \{\delta c(\Delta)\} = \text{Var} \left\{ c_o \left[1 - \frac{0.83 \quad U \frac{h,m}{10m}}{k_R^2 a^2 \delta^2 \quad (1 + \frac{d,m}{10m}} \right] \right\} \tag{27}$$

or

$$\sigma_{\delta c}(\Delta) = \left[\frac{0.83 \, U c_o}{\left(k_R a\right)^2 \left(1 + \frac{d,m}{10m}\right) \delta^2} \right] \sigma_{h/10} \tag{28}$$

where $\sigma_{\delta c}(\Delta)$ = rms value of fluctuations in sound speed due to perturbations of bubble resonant frequency.

$\sigma_{h/10}$ = the dimensionless fraction, rms height of surface wave in meters/10 meters.

Since we are dealing here with very slowly varying surface heights ($F < 1.$ Hz) the change of resonant frequency and radius of the bubble will occur with negligible phase lag. Therefore, equation (25) can be viewed from the point of view of a sinusoidal change of height, $h,m = H,m \sin \Omega t$

where $\Omega = 2\pi F$

and F = a component of the surface wave spectrum causing a simultaneous change of Δ in equation (25) and of the differential sound speed without phase change at the same driving frequency. In the case of a spectrum of surface height, equation (28) can be rewritten

$$\delta c(\Omega)d\Omega = \frac{0.83\ Uc_o}{\left(k_R a\right)^2\left(1 + \frac{d,m}{10m}\right)\delta^2} H(\Omega)d\Omega \qquad (28a)$$

C. Theoretical Basis for the Experimental Measurements

The physical form of the acoustic sound path is shown in Figures 3 and 4. Sound from the piston-like transducer propagates through the frame and the sound pressure is measured by a series of very small "identical" hydrophones along the path. For a plane wave, or in the far field of the piston, the phase shift along the distance, x, between two hydrophones is measured by counting the integral number of wave lengths, n, and determining the residual phase angle, ϕ, which represents the instantaneous fractional wave length, $\phi/360$. Then the instantaneous speed is calculated by the product of frequency by wave length, using

$$c = \frac{fx}{n + \phi/360} \qquad (29)$$

The assumptions in the derivation, as well as the accuracy of the component measurements, are discussed in reference 11.

IV. EXPERIMENTAL DETAILS

A photograph of Kingfish A Tower is presented in Figure 2. A rectangular aluminum pipe frame of height six feet and length eighteen feet, was used to mount the transducers, hydrophones, flowmeter, velocimeter and thermister (Figs. 3 and 4). To prevent displacement of the hydrophones, the hydrophone mounting wires were put under tension and isolated from the frame by rubber shock mounts. To minimize any reflections from the frame, selected segments were covered with acoustic absorbent rubber (SOAB). See also references 11 and 14.

The rectangular frame was hung so that the sound source and receivers were in a horizontal line. The method of attachment to a nominal 45° steel cable is shown in Figure 4. The steel cable had one end held to the ocean floor by an anchor, the other end was fixed to the tower. The steel cable and polypropylene attachment lines can be seen in Figure 2 and to the right in Figure 3 as they enter the water.

At the center of one end of the frame, pointing in the horizontal (X) direction, an USNRD F-33 piston transducer was mounted. On the acoustic axis of this transducer, four Atlantic Research LC-10 hydrophones were placed at source separations shown in Table 1.

TABLE 1.

SOURCE TO HYDROPHONE SEPARATIONS (METERS)

	BASS I	BASS II
LC 10-1	1.047	1.065
LC 10-2	0.998	0.988
LC 10-3	2.002	1.990
LC 10-4	1.355	0.986

Fig 2. Photograph of the platform, Kingfish A, from which the experiments were conducted.

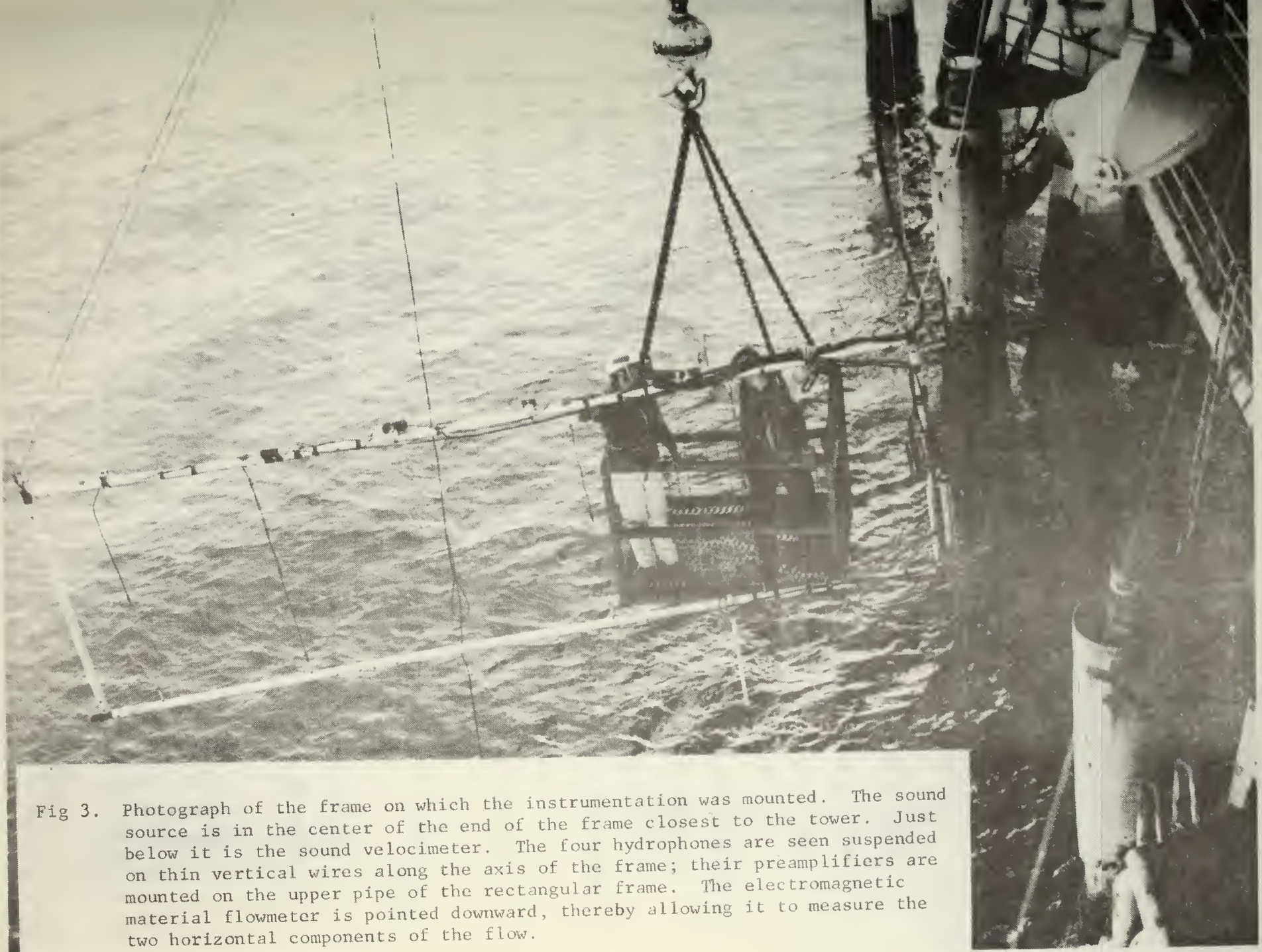

Fig 3. Photograph of the frame on which the instrumentation was mounted. The sound source is in the center of the end of the frame closest to the tower. Just below it is the sound velocimeter. The four hydrophones are seen suspended on thin vertical wires along the axis of the frame; their preamplifiers are mounted on the upper pipe of the rectangular frame. The electromagnetic material flowmeter is pointed downward, thereby allowing it to measure the two horizontal components of the flow.

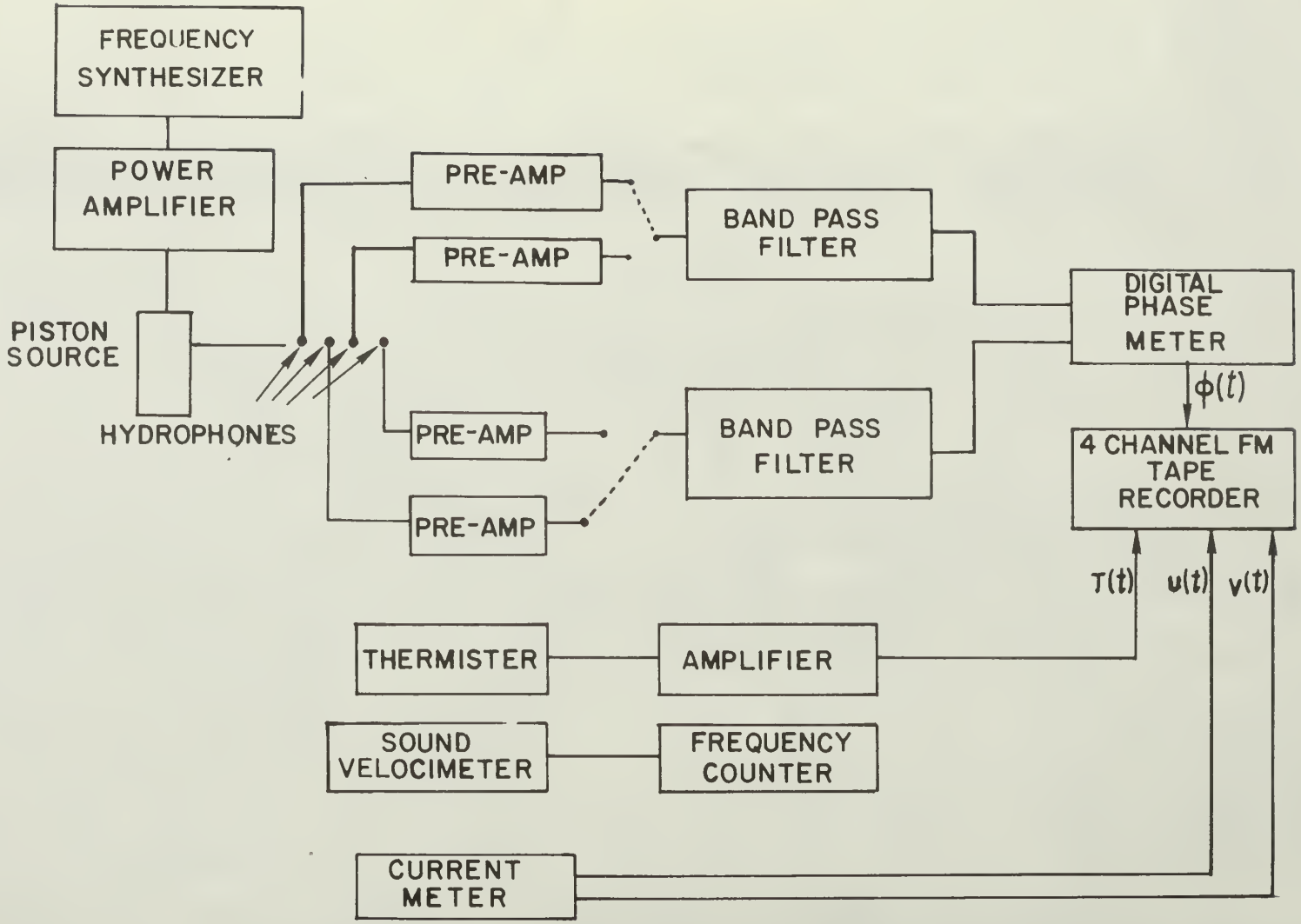

Fig 4. Sketch of equipment frame and components.

The transmitting instrumentation (Figure 5) consisted of a General Radio coherent decade frequency synthesizer, type 1162-A, generating a stable sinusoidal output of two volts rms, selectable in frequency. The signal was amplified by a Hewlett-Packard Power amplifier, 467A, to voltage levels consistent with undistorted signals through the receiving instrumentation, and then impressed across the transducer.

The receiving instrumentation (Figure 5) consisted of four LC-10 hydrophones with flat (-110dB ± 3 dB re 1 volt/microbar) receiving responses from 10 kHz to 150 kHz. The signals from the hydrophones were amplified 30 dB by NUS pre-amplifiers (model 2010-30) before passing through 180 feet of water-proof shielded cable. Two selected signals were then bandpass filtered by digitally tuned variable Krohn-Hite model 3322 filters (down 24 dB/octave outside of band) set with the center frequency equal to the transmitted frequency ± 300 Hz. The filtered signals were then fed into a Dranetz model 305 phase meter. The phase meter measured the phase angle between the two ac voltages and provided a dc voltage output (10 ms response time) proportional to the difference of the phase angles at 10 mv per degree. The dc voltage was FM recorded at 3.75 ips on a Precision Instrument model 2101, seven track magnetic tape recorder.

The thermister was mounted on the frame midway between the first two hydrophones. The dc voltage output was FM recorded at 0.5 v per degree C.

The reference sound speed was obtained by an NUS model 2030 - 103 - 12 velocimeter operating at 3MHz transmit frequency. The frequency output was time averaged and manually recorded. The frequency output was also demodulated to produce a time varying dc voltage which was FM recorded at 20.48 mv per m/sec sound speed.

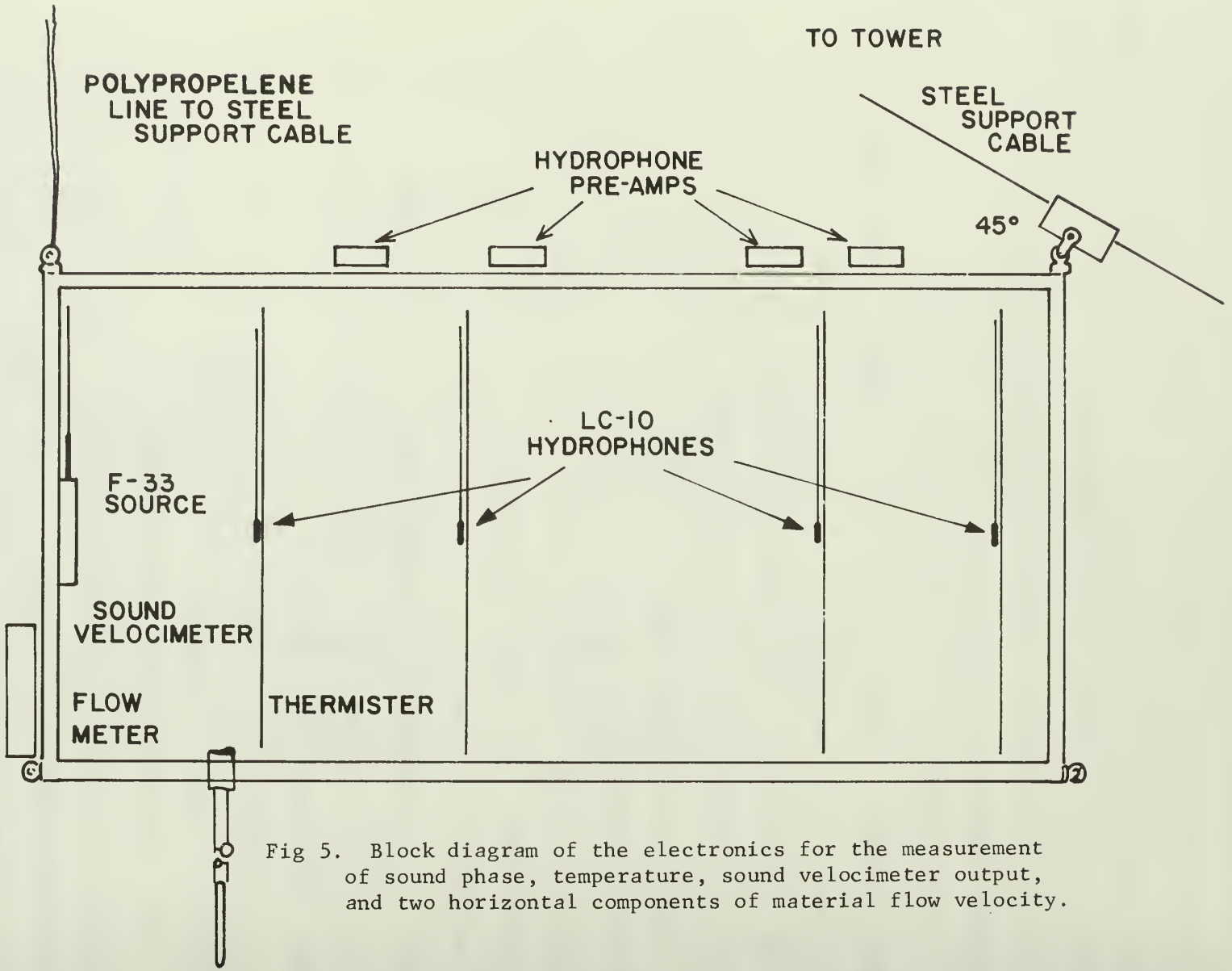

Fig 5. Block diagram of the electronics for the measurement of sound phase, temperature, sound velocimeter output, and two horizontal components of material flow velocity.

Two orthogonal horizontal components of the water particle velocity were determined by the mounting of an EPCO water current meter such that the velocities measured corresponded to the direction of acoustic propagation of the USNRD F-33 transducer and the transverse or Y direction (BASS II). These two outputs were also FM recorded at 1.640 volts per M/sec.

V. DATA PROCESSING

Data processing was essentially the same as described in previous Naval Postgraduate School reports (Refs. 11,14). See Figure 5.

A series of ten minute and four minute individual records makes up the analog recorded time varying sound phase difference, water current components, temperature, and velocimeter data. The approach used was to digitize the analog data and use a computer to carry out the statistical correlation and spectral analysis.

The recorded data were digitized using the Royal Australian Naval Research Laboratory's PDP-11 computer. The sampling frequency was 6.4 Hz, giving a Nyquist frequency of 3.2 Hz. The sampling interval was 0.15625 seconds and the frequency resolution was 0.05 Hz. The analog signals were low-passed filtered at 3.2 Hz, scaled and written on magnetic disk. The horizontal beam (X) direction component of water current was scaled to meters per second. For each instantaneous value of phase, the instantaneous value for the speed of sound was calculated, in meters per second, and instantaneous value for water current in the X direction was algebraically subtracted to correct for apparent sound velocity due to the motion of the medium with respect to the sound field.

The mean values, variances and standard deviations were then determined.

The mean speed was then compared with the mean speed values given by the NUS Velocimeter.

The temporal autocorrelations were computed and plotted using a maximum time lag of 20 seconds. The temporal cross correlation was also computed between sound speed and water cross current, and sound speed and temperature. From these, the auto-spectrum was computed.

VI. ANALYSIS OF RESULTS

A. Average Speed of Sound as a Function of Depth

The equipment used for the phase comparison determination of the speed of sound is capable of yielding values with an absolute error of less than one meter per second[11], provided that corrections are made for ocean currents and the small phase difference between the hydrophone-preamplifier electrical responses. Column 3 of Table 2 presents the values of the average sound speed $\langle c \rangle$ determined by our phase comparison method, corrected for ocean current, at two frequencies, 24.4 and 95.6 kHz (BASS II). Hydrophone separation was 0.988 m. Column 4 presents the concurrently read and averaged values of the mean speed $\langle c_o \rangle$ given by the sound velocimeter. In column 5, we take the difference between column 3 and 4 in order to arrive at the differential velocity, $\Delta c = \langle c \rangle - \langle c_o \rangle$. These values are due to bubbles plus a correction for the previously mentioned hydrophone electrical phase difference. A complete frequency run at depths great enough to validate the assumption of a no-bubble region at 13.7 m was not concluded because of the failure of the tape recorder. However, from the evidence of the standard deviation of sound speeds shown in Table 3, it is quite convincing that the depth of 13.7 m can be used to represent the bubble-free medium, and,

TABLE 2

BUBBLE FRACTION AND AVERAGE SOUND SPEEDS

AT FREQUENCIES 24.4 AND 95.6 kHz AS A FUNCTION OF DEPTH

BASS II

Depth Z Meters	$\beta = 1.33/(1+0.1Z)$	$\langle c \rangle$ M/sec	$\langle c_o \rangle$ M/sec	$\Delta c = \langle c \rangle - \langle c_o \rangle$ M/sec	$\delta c = \Delta c_z - \Delta c_{13.7m}$ M/sec	U ($\times 10^{-7}$)
Frequency 24.4 kHz						
3.0	1.0	1506.0	1522.1	16.1	− 1.8	1.9
4.6	0.91	1506.4	1522.2	15.8	− 2.1	2.5
6.1	0.83	1506.7	1522.2	15.5	− 2.4	3.2
7.6	0.76	1505.9	1521.9	16.0	− 1.9	2.7
13.7	0.56	1504.3	1522.2	17.9	0	0
Frequency 95.6 kHz						
3.0	1.0	1514.2	1521.6	7.4	− 2.5	-
4.6	0.91	1513.6	1521.7	8.1	− 1.8	-
6.1	0.83	1513.4	1521.9	8.5	− 1.4	-
7.6	0.76	1512.8	1522.1	9.3	− 0.6	-
13.7	0.56	1512.3	1522.2	9.9	0	-

$\langle c \rangle = \langle c(f) \rangle_f$ = time average value of sound phase speed by phase comparison.

$\langle c_o \rangle$ = time average sound phase speed by velocimeter (at 3 MHz).

therefore, to correct for the hydrophone-preamplifier electrical phase shift. This has been done to arrive at column 6 of Table 2, the corrected differential speed of sound due to bubbles, $\delta c = \Delta c_z - \Delta c_{13.7}$. Finally, column 7 gives the average bubble fraction, U, calculated from equation (11), using average values.

The frequency 24.4 kHz was selected because it was the lowest frequency available with the 35 dB S/N ratio required for accurate phase information. The values of the corrected differential speed become more negative (down to 6.1 M) as depth is increased, presumably because there is a peak bubble population just above 24 kHz at surface level which increases its resonant frequency to higher values with increasing depth. A strong population sweeping by the sound frequency of 24.4 kHz would cause larger negative values of δc. Finally, however, by 7.6 m depth, the decreasing numbers of bubbles becomes the dominant factor and the speed approaches the no-bubble value.

The frequency 95.6 kHz presents a continuously decreasing value of δc as depth increases. Reference 14 shows that there is a trough of sound speed at this frequency, caused by the larger number of bubbles at higher resonant frequency. As the depth is increased, existing large bubbles have increasingly high resonant frequencies which produce a positive increment to add to the speed of sound, thereby reducing the negative corrected fifferential speed as the depth is increased. The smaller number of bubbles at greater depths acts, also, to bring the value of δc closer to zero.

The ratio of the average change in sound speed ascribable to bubbles, δc, to the average speed in non-bubbly water $\langle c_o \rangle$ (equivalent to the velocimeter reading at 3 megahertz) is plotted in Figure 6 as a function of the pressure parameter, $\beta = 1.33(1 + 0.1\ z)$. In reference 15 it was shown that

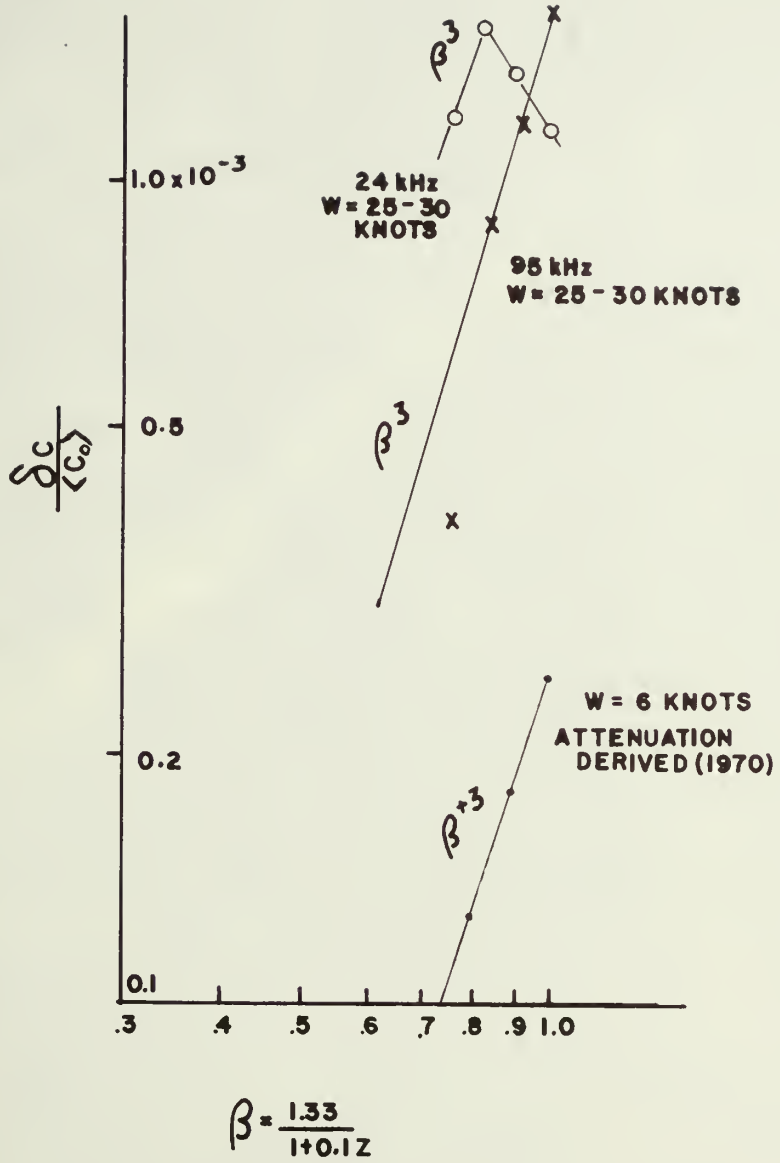

FIG 6 Variation of the relative change of speed due to bubbles, $\delta c/\langle c_0 \rangle$ as a function of the pressure parameter, $\beta = 1.33/(1+0.1\ Z)$ where Z = depth in meters. The data of this experiment, at 24.4 and 95.6 kHz, measured during winds speeds of 25-30 knots, are compared with previous attenuation derived data obtained during wind speed 6 knots.

the ratio $\delta c/\langle c_o \rangle$ behaved as β^{+3}. That deduction was based on attenuation measurements performed at wind speeds of 6 knots. The slope is plotted in Figure 6 for comparison with the present data. It appears that both the 24.4 and 95.6 kHz data approximately follow that same depth dependence except for the contrary slope due to the previously mentioned 24.4 kHz resonant bubbles nearer the surface. It is interesting, also, to compare the magnitudes of the bubble effect, as a function of wind speed. This is possible if one assumes that the waters in BASS Strait are biologically similar to those off San Diego, and that the cause of the sound speed difference is bubble presence due to the greatly different wind speed. The ratio of the differential sound speeds is approximately 6 to 1, which is close to the wind speed ratio of the two experiments (28 knots to 6 knots). Therefore, the proportionality of volume fraction and differential sound speed to wind speed, assumed in reference 15, is roughly verified here. More data of this type are needed to determine whether the simple proportionality is indeed correct and, if so, the limit of this proposed law.

B. Average Speed of Sound as a Function of Sound Frequency

The dispersive effect of ambient bubbles at sea has been predicted on the basis of excess attenuation measurements[15], and has been measured directly in two previous experiments[11,14]. Although an attempt to repeat the ambient experiment in BASS Strait was frustrated by the tape recorder failure in BASS II, data of special interest with respect to bubbles near structures was obtained during BASS I. The previously discussed electronic phase shift, measured in BASS II, and smoothed between 24 and 96 kHz was used to reduce the data. A photograph of the frothy surface of the water next to the tower docking area and about 5 meters above the measuring equipment is shown in Fig. 7

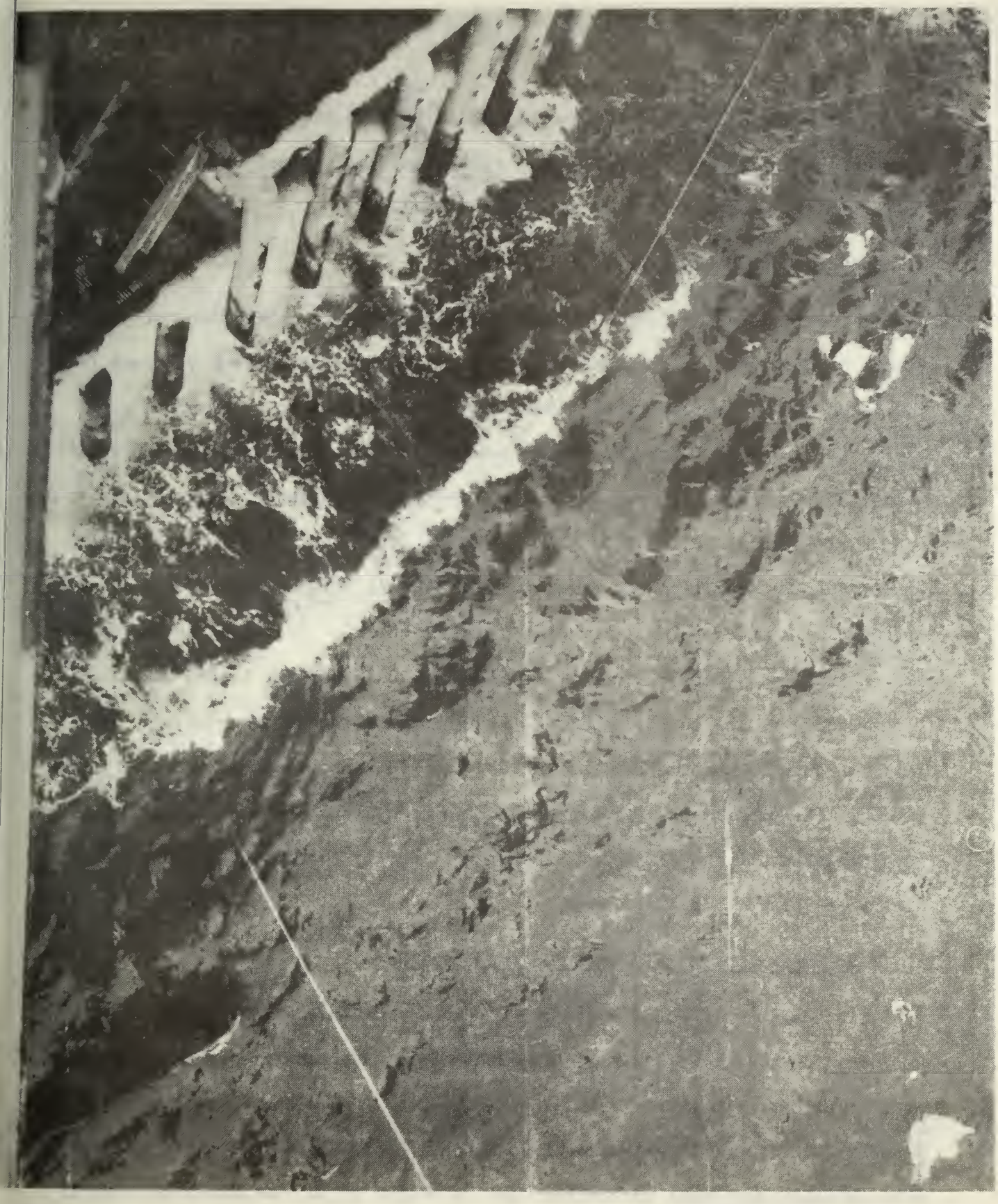

Fig 7. Photograph of the ocean surface at the base of the tower during the data collection for the graph of Fig 8. The equipment is at depth 15 feet, next to the tower.

The sound speed dispersion is shown by solid line in Figure 8. The curve of reference 14 is shown by dashed line. The peaks and troughs of differential speed are the greatest that we have ever determined.

C. Average Bubble Fraction

The estimated asymptotic differential speed of -15 meters/sec, of Figure 8, when used in conjunction with equation (11) of section 3, leads to the value of the average total fractional volume of gas in bubble form to water, $U = 1.2 \times 10^{-6}$ for the region near the tower. This value is approximately 30 times the fraction for ambient bubbles found at 3.3 m depth in a 6 knot wind condition, 10 times the values at depths to 7.6 m in the 28 knot wind (Table 2) away from the tower in BASS II, and 6 times the value measured directly by microscope near breaking waves at shore[4]. One might suspect that the optical measurement, since it is effective only for the larger bubbles, underestimates the total fraction. It is interesting to observe that the peaks of sound speed are at frequencies close to those found in previous work although the experimental frame and particular hydrophones and preamplifiers were different in the different experiments, partly to eliminate the possibility of instrumental artifacts.

D. Fluctuations of Bubble Fraction and Sound Speed

Fluctuations in sound speed may be caused by fluctuations in temperature, salinity, depth, fraction of gas in bubble form, resonant frequencies of bubbles or distribution of bubbles with radius. From a consideration of Wilson's equation for the speed of sound in a bubble-free region, it is clear that salinity and depth variations (due to change of sea surface displacement with time) are generally quite unimportant compared to the temperature varia-

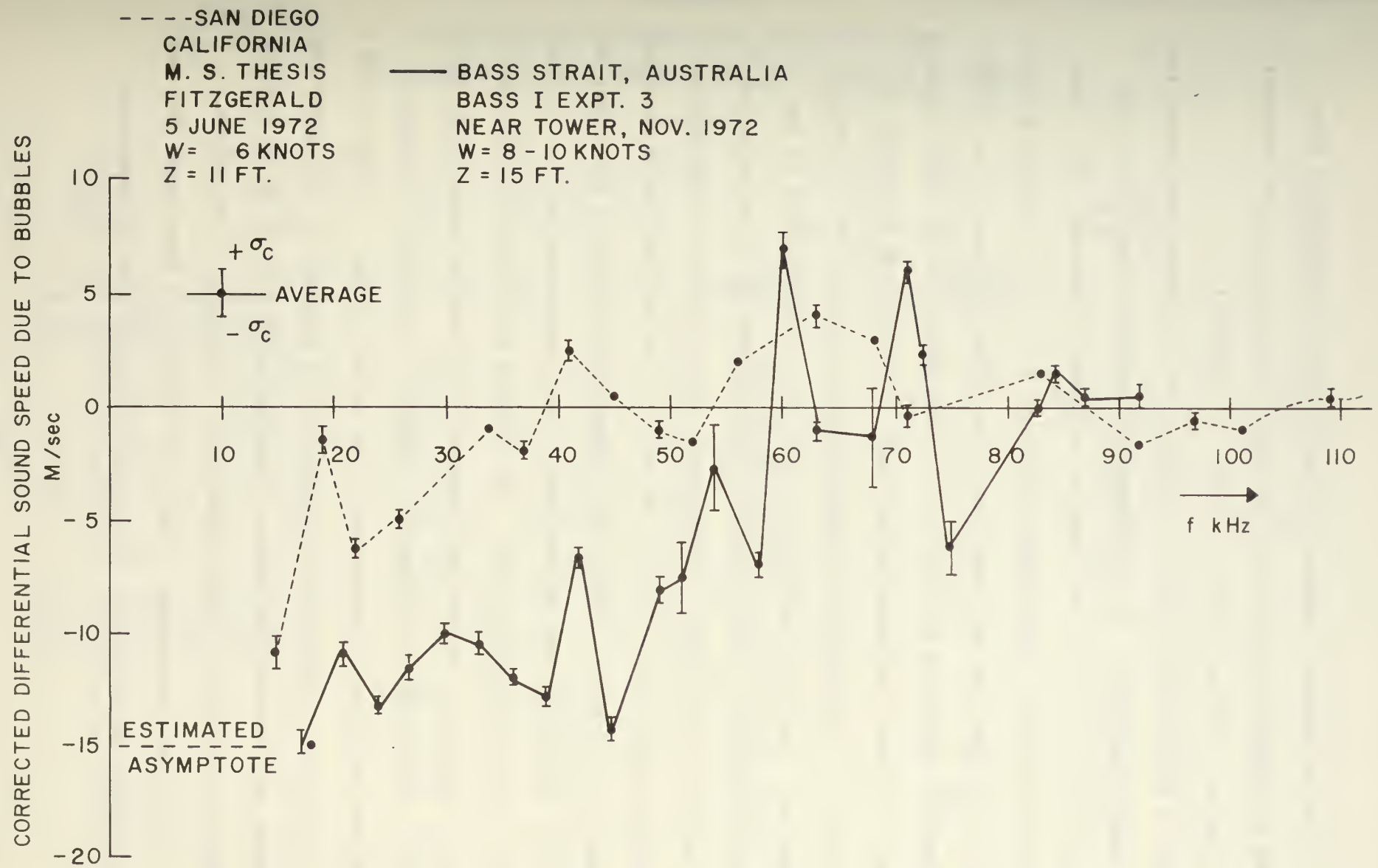

Fig 8. Differential sound speed due to bubbles as a function of sound frequency. Two sets of results are shown: the dashed line represents data of an experiment from the NUC tower at a depth of 11 ft in 55 ft of water, one mile offshore suring wind speed 6 knots. The solid line shows data of BASS I at depth 15 ft, during wind speed 8-10 knots and clear visual evidence of bubbles generated at the adjacent tower structure. The standard deviations are indicated by vertical bars of height $\pm \sigma_c$.

tions. It is of interest, however, to compare the fluctuations of sound speed due to temperature variation with those attributable to the different bubble effects. This can be done by means of equation (19).

Table 3 displays the results of calculations of fluctuations during the BASS II depth experiment. The experiment was conducted from 1110 to 1255 (24.4 kHz) and 1255 to 1442 (95.6 kHz) on Saturday, 17 February 1973. The equipment was lowered to five depths, 3.0, 4.6, 6.1, 7.6, 13.7 m, at a location about 100 feet from the tower, which was evidently free of tower effects. The hydrophone separation was 0.99 m. The wind speed of 25-30 knots measured at height 37 m above the ocean surface leads to a predicted rms height of waves, σ_H = 1.1 m, assuming the Pierson-Moskovitz spectrum for the fully developed sea. This wind had persisted for about 24 hours prior to the acoustics experiment. A swell wave of estimated peak to trough height of 2 meters appeared to be present. Under these conditions the rms variation of the average speeds of sound at 24.4 kHz and 95.6 kHz at five depths are given in column two of Table 3. Column four presents the calculated rms values of c_o which is calculated from the variance of the temperature and the constant, b, of the linearized equation (15). The variance of the excess speed due to bubbles is obtained by subtraction (equation (19)) and its square root, the rms value, is presented in column five, "EXPT". It is seen to be greater than the rms value due to temperature, (see footnote Table 3) except for 95.6 kHz at the greatest depth of the experiment, 13.7 m, where we can assume that the bubble population is negligible. Since variances add, it is appropriate to compare the variance of sound speed due to temperature fluctuations, Var $c_o = \sigma_{c_o}^2$, as a percentage of the total variance of sound speed fluctuations, as shown in column six. The relative variance due to temperature

TABLE 3

FLUCTUATIONS OF TEMPERATURE AND SOUND SPEED

AT FREQUENCIES 24.4 AND 95.6 kHz AS A FUNCTION OF DEPTH

BASS II

Depth Meters	σ_c M/sec	σ_T °C	$\sigma_{c_o} = (b^2 \text{ Var } T)^{\frac{1}{2}}$ M/sec	$\sigma_{\delta c} = (\text{Var } c - b^2 \text{ Var } T)^{\frac{1}{2}}$ M/sec		$\frac{\text{Var } c_o}{\text{Var } c}$ %	σ_U ($\times 10^{-7}$)
				EXPT	THEORY		
Frequency 24.4 kHz							
3.0	1.27	0.068	0.18	1.26	-	1%	0.57
4.6	4.01	0.038	0.10	4.00	-	0.02%	0.71
6.1	3.16	0.040	0.11	3.16	-	0.1%	0.44
7.6	2.77	0.050	0.13	2.76	-	0.2%	0.33
13.7	0.19	0.052	0.14	0.13	-	55%	-
Frequency 95.6 kHz							
3.0	0.56	0.25*	0.18	0.53	7.5	10%	-
4.6	0.61	0.31*	0.10	0.60	7.6	3%	-
6.1	0.35	0.29*	0.11	0.33	8.3	10%	-
7.6	0.26	0.23*	0.13	0.23	5.5	25%	-
13.7	0.089	0.19*	0.14	0	-	100%	-

See following page for footnotes and explanation of terms

TABLE 3 (Cont.)

c_o = speed of sound measured by velocimeter = speed predicted by Wilson's equation

= $c_r + bT$ in the linearized form for temperature, T.

c = speed of sound measured by phase comparison = $c_o + \delta c$

$\overline{\sigma}_c$ = standard deviation of excess speed of sound due to bubbles

$\overline{\sigma}_T$ = standard deviation of temperature fluctuations

δc = excess speed of sound due to bubbles

c_r = reference speed of sound in the linearizing equation for temperature

b = constant in the linearizing equation for temperature

*These absolute values of $\overline{\sigma}_T$ at 95.6 kHz were contaminated by a slow drift during recording. The values of $\overline{\sigma}_T$ at 24.4 kHz are used for these calculations

fluctuations is particularly small at the frequency 24.4 kHz, and particularly large at both frequencies at the greatest depth due to the deficiency of bubbles there. The distinction between the two frequencies will be discussed later after we have looked at the temporal correlations.

Finally, the standard deviation of fluctuations of the bubble fraction is shown in the last column for the 24.4 kHz sound, where a calculation is possibly by using equation (20). The standard deviations, σ_U, range from one-third to one-eighth of the average bubble fractions themselves, U, given in Table 2.

If one has the situation: (a) the variance of sound speed due to temperature fluctuations is negligible and (b) the variance of sound speed is principally due to perturbation of the resonant frequency of bubbles, it is possible to use equation (28) to estimate the rms value of the excess speed of sound fluctuations. Assumption (a) is verified by column six of Table 3, except, of course, for the greatest depth, 13.7 meters. Assumption (b) would be applicable only if we are considering a sound frequency at which there is a very large population of bubbles. Such a situation can be identified either by a large excess absorption, a large excess speed of sound, or a large cross correlation between the sound phase and the surface wave height, such as was observed in reference 14. The cross correlation test is the best criterion to use but, unfortunately, surface wave heights were not recorded in this experiment. In section F we will show that at 95.6 kHz the phase fluctuation spectrum is highly responsive to the surface wave height spectrum. This is pretty good evidence of a strong bubble population resonant to 95.6 kHz, so we have proceeded on that assumption.

The parenthetical inserts of Column 5 of Table 3, presents the results

of our attempt to use the simple linear theory (equation (28)) to predict $\sigma_{\delta c}$, the rms value of the speed fluctuations due to bubbles for the frequency 95.6 kHz. Comparison with the experimental values of column 5 shows that our predictions are an order of magnitude too large. It is not difficult to find the reason for this overestimation. The flaw is that we have used our simple theory (equations 21-28) which was developed for a single radius population with $\Delta < 0.05$ in attempting to predict frequency swings that were as great as $\Delta = 0.16$ in a multiradius population in the high seas of BASS II. The theory overestimates the magnitude of the speed fluctuations because it uses the slope near $f_R = f$ for the calculation, when, in fact, this slope is the maximum slope and is applicable only for bubbles of precisely $f = f_R$. For bubbles slightly off resonance and for larger excursions of pressure, the changes are very much less. Furthermore, for very large excursions in pressure, the phase shift becomes "counterproductive" because the sections of the dispersion curve over the hump start to produce phase shifts that cancel the effect near $f_R = f$. We believe, therefore, that the order-of-magnitude disagreement between the experimental and theoretical parts of column 5 are not a contradiction of our theory of the probable cause of the speed fluctuations at 95.6 kHz. Additional confirmation follows in section F.

E. Temporal Correlations

The tentative conclusions about the acoustical effect of bubbles, which we obtained by consideration of the variances, are reinforced when we consider the temporal correlations. Consider Figure 9, which shows the temporal correlations of the temperature at the four depths, 3.0, 4.6, 6.1

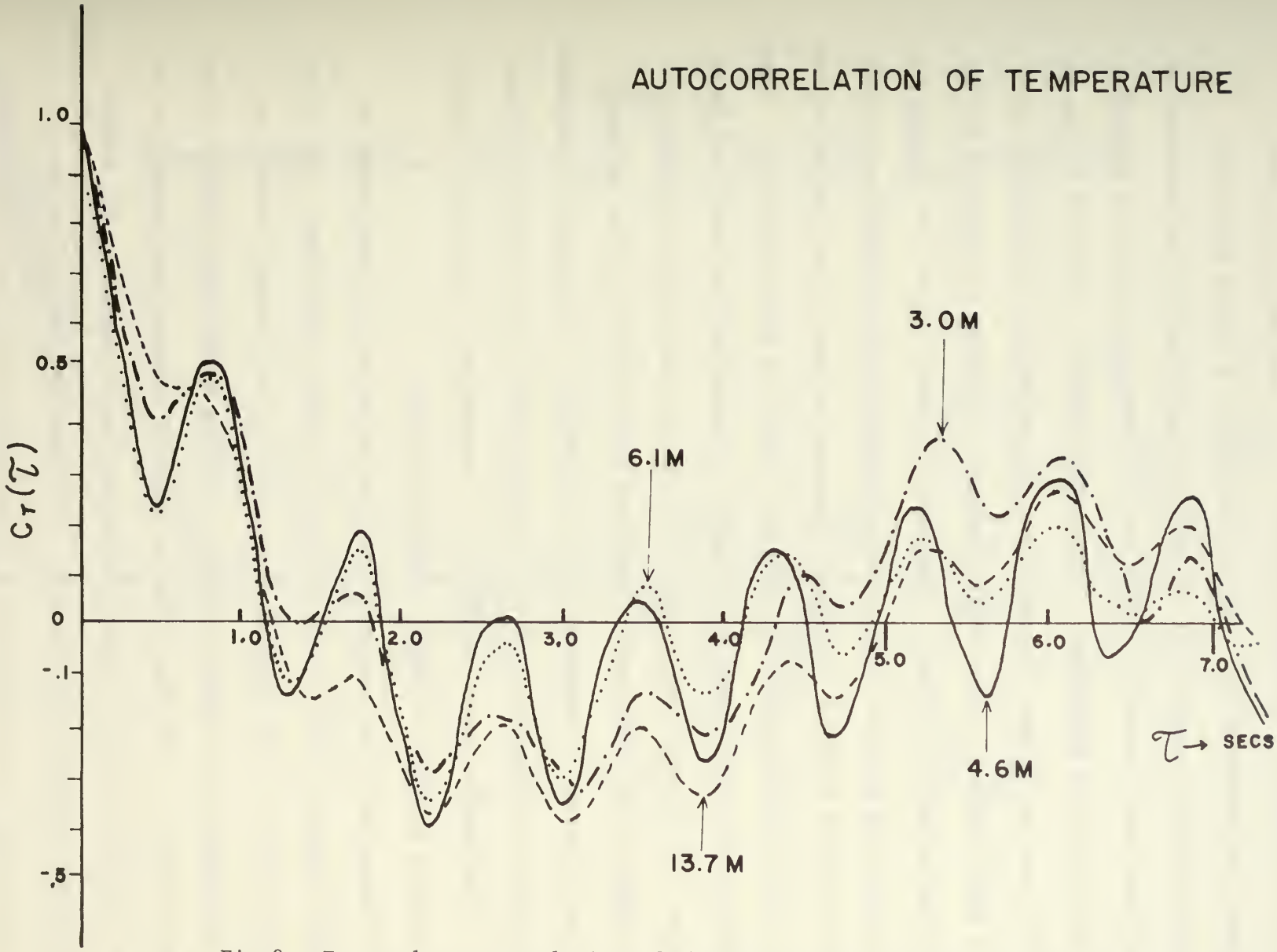

Fig 9. Temporal autocorrelation of the temperature fluctuations at depths 3.0, 4.6, 6.1, and 13.7 m. Measurements made during 24.4 kHz sound phase study, BASS II.

and 13.7 m during the 24.4 kHz run. The gross appearance is of an exponential or Gaussian correlation function with a periodicity of about 6 seconds (see reference 18). This corresponds to a narrow band noise centered around a peak at 0.16 Hz, which is approximately the frequency at which peak energy density is found for the wind wave system that existed at the time of the experiment. It is noted that the correlation period is a little shorter (higher frequency) for the temperature fluctuations at 3.0 m depth compared to the greater depths; this would be accounted for by filtering action due to depth. That is, at greater depths, the frequency spectrum of the particle velocities associated with the surface wave system will be shifted toward a lower peak frequency because of the greater attenuation and, therefore, the more effective removal of high frequencies. Superimposed on the large period variation is a correlation periodicity of about 1 second. We believe that this fine structure is an artifact produced by oscillation of the cable and/or the frame which held all of the equipment. The fine structure is repeated in all the records of temperature, components of velocity, and phase at 13.7 m. We believe that this fluctuation exists also in the phase at other depths but is overwhelmed by the bubble effects that we were studying at nearer surface positions.

Turning now to the temporal autocorrelations of the sound phase, we consider Figures 10 and 11, for 24.4 and 95.6 kHz, respectively. In Figure 10, we see that, at the greatest depth, 13.7 m, the temporal correlation of the sound phase at 24.4 kHz is almost a replica of the temperature correlations of Figure 9. The fine structure appears with the same periodicity of about 1 second, and the 6 second periodicity due to motion of the surface wave system is clearly seen as well. Recalling our analysis of the

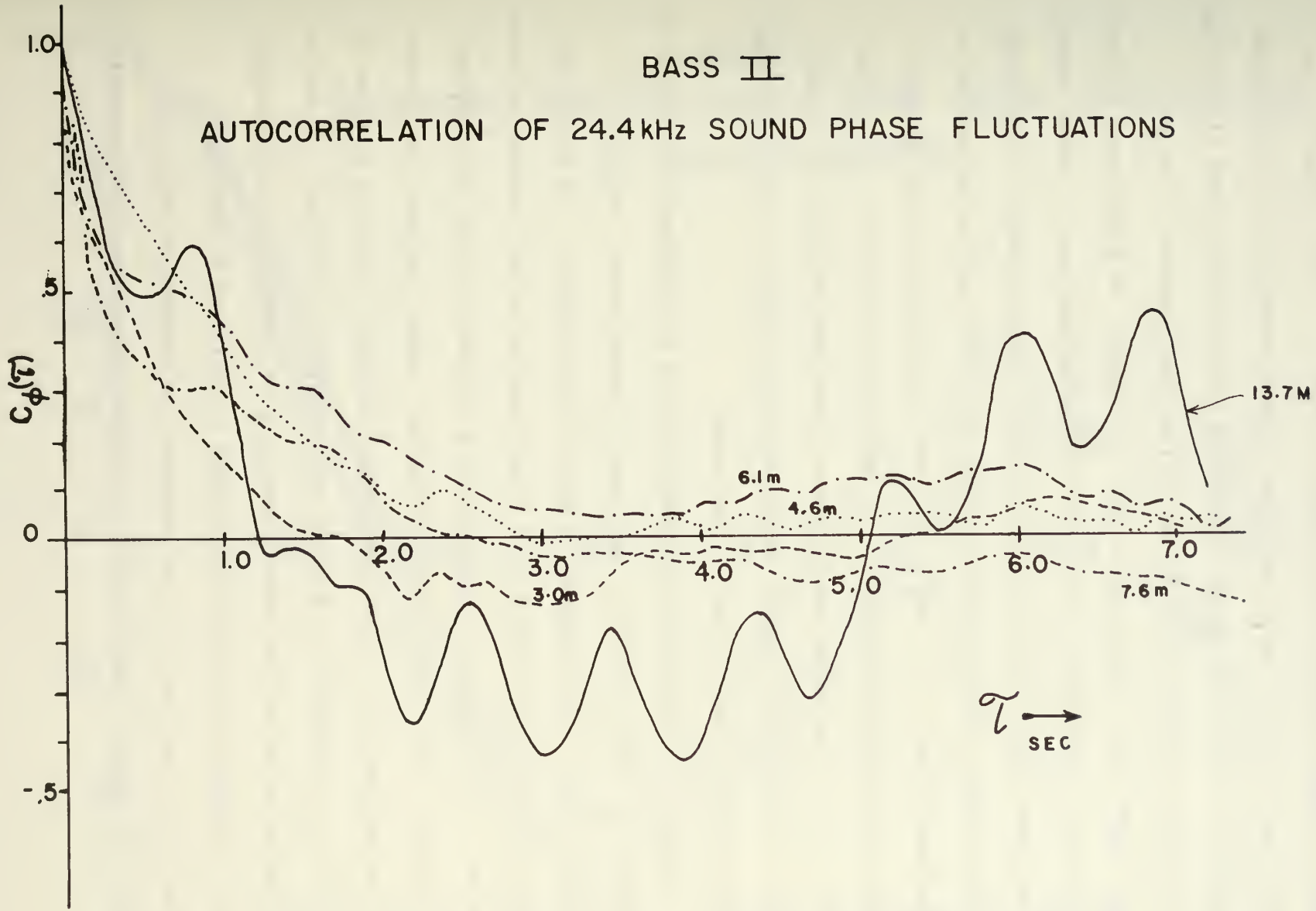

Fig 10. Temporal autocorrelation of phase fluctuations for 24.4 kHz sound at depths 3.0, 4.6, 6.1, 7.6 and 13.7 m. BASS II.

variances, this is a case in which the temperature-caused variance of the speed is greater than the bubble-caused variance. It is, therefore, not surprising to find the sound phase correlation resembling the temperature correlation at 24.4 kHz as the temperature microstructure moves with respect to the frame. There is only a hint of the fine structure at the depth 7.6 meters where Table 3 has shown us that the variance of sound speed fluctuations due to temperature is only 0.2% of the variance due to bubble effects. At shallower depths there is even less fine structure because, even though the frame moved, the phase fluctuations were due to bubbles rather than to temperature blobs. It is our belief that the decorrelation of the sound phase at all depths except 13.7 m is principally a measure of the randomness of the strong bubble populations at these nearer-surface positions. There is virtually no response to the ocean wave system at the near-surface positions in the case of the 24.4 kHz sound.

Figure 11, the temporal autocorrelation of sound phase fluctuations at frequency 95.6 kHz presents a completely different story. Only at 13.7 m is there a hint of the temperature-motion fine structure. The predominant general feature is the narrow band noise character of the correlation function with a periodicity of approximately 6 seconds, that is, the frequency 0.16 Hz again, the center of the surface wave energy spectrum. We propose that the explanation of these correlation functions, which are so close to what is to be expected of a surface wave correlation function[23], is due to the responsiveness of the resonant frequency of predominant bubble populations to surface wave pressure variations as explained in Section III, B, and as used in Section VI, D, to calculate the theoretical variance in Column 5 of Table 3. We do not have the directly measured bubble distribu-

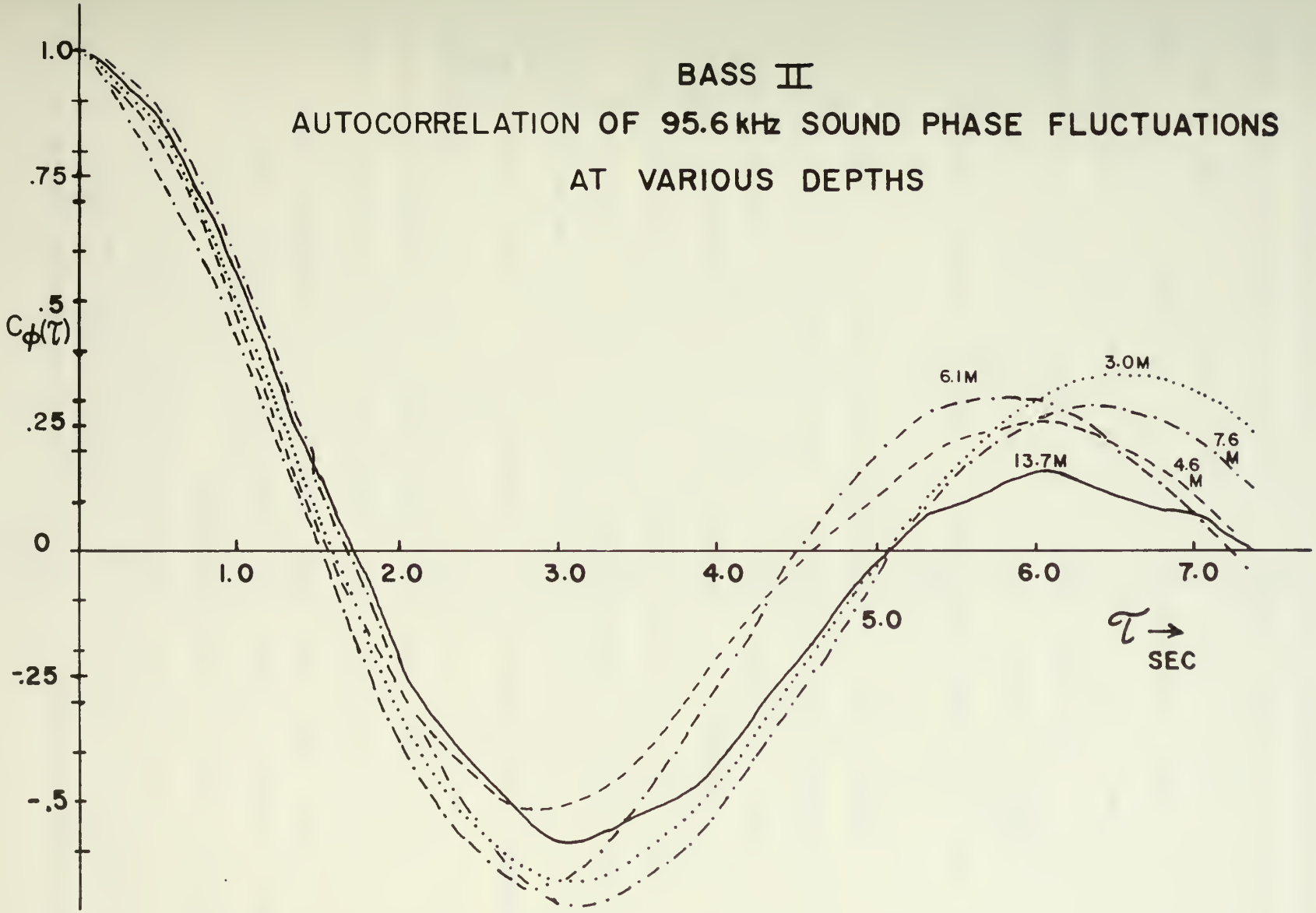

Fig 11. Temporal autocorrelations of phase fluctuations for 95.6 kHz sound at de ths 3.0, 4.6, 6.1, 7.6 and 13.7 m. BASS II.

tions to prove absolutely that there was a large bubble population resonant at 95.6 kHz at all depths. However, it should be recalled that the resonant frequency is proportional to the 5/6 power of the ambient pressure. This means that a large bubble population resonant at frequency f_o at depth 3.0 m will be resonant at $2f_o$ at 18 m. Therefóre, it should not be surprising to find effects of large bubble populations, resonant at 95.6 kHz, at all depths of this experiment conducted in a sea churned up by 25-30 knot winds. In fact, there is ample ancillary evident of a large population of bubbles at 95.6 kHz, as will be seen in Section F.

Two temporal cross correlations have been plotted in an attempt to further characterize the effect of the medium on the sound phase. Figure 12 shows the cross correlation of flow velocity fluctuations (the axial component of the velocity of the water with respect to the frame and sound field axis) and 24.4 kHz sound phase variations. It is observed that the long term periodicity of 6 seconds is again found for both 3.0 m and 13.6 m depths, but the fine scale fluctuation of approximately 1 second periodicity is clearly identifiable only at the greater depth. The fact that the fine structure is almost non-existent on the correlogram for 3.0 m is presumably due to the very much larger peak frequency orbital flow velocity components which will tend to swamp the other temperature-caused fluctuations of sound phase variation after normalizing. Figure 13 is a correlogram of the temporal correlation of flow with temperature. It is almost identical to the previous figure for the same reasons.

It is observed that the correlation envelopes at 95.6 kHz require much more time to decay than their counterparts at 24.4 kHz, particularly the shallow depth correlograms at 24.4 kHz. The interpretation that we make is

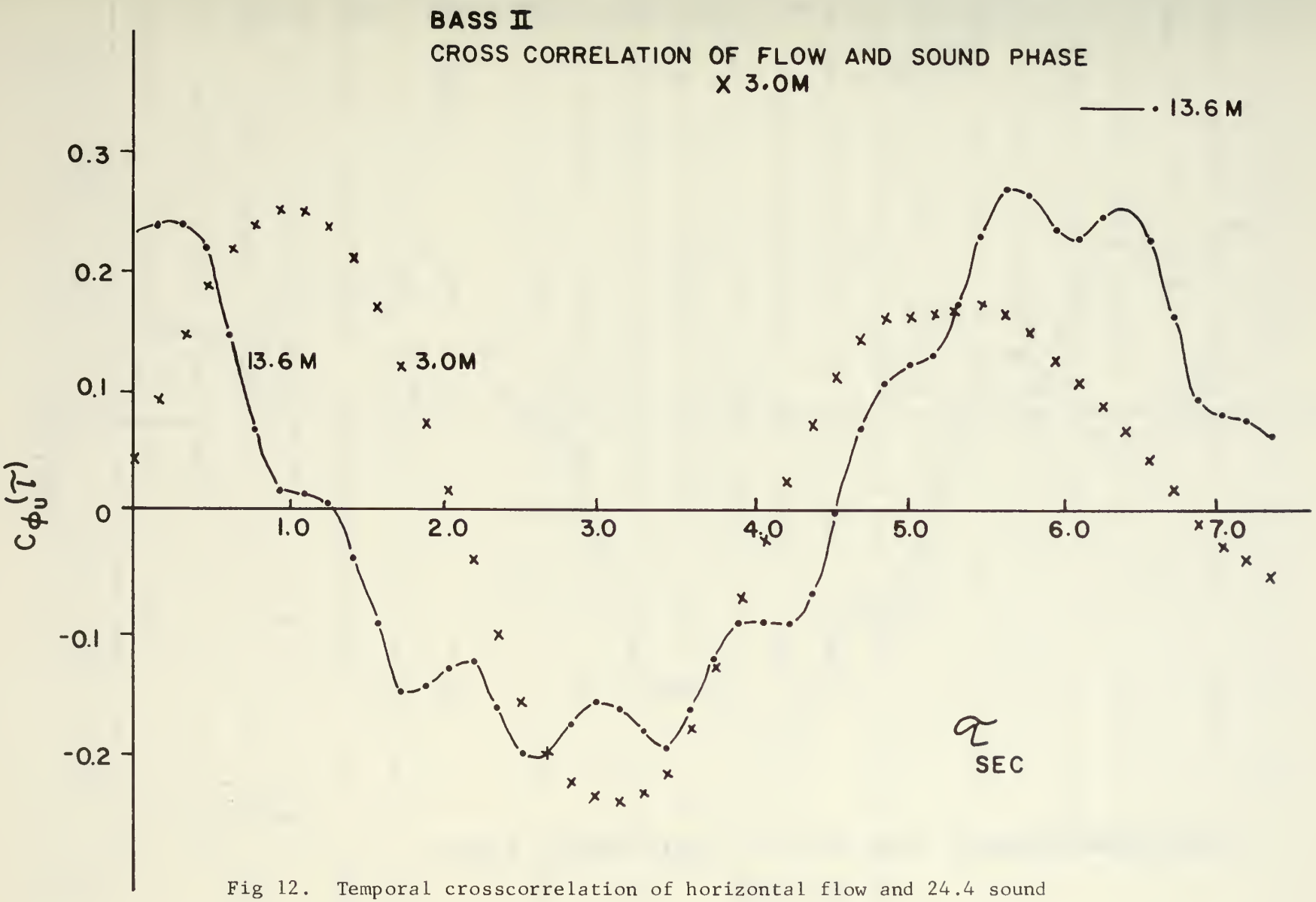

Fig 12. Temporal crosscorrelation of horizontal flow and 24.4 sound phase at depths 3.0 and 13.7 m. BASS II.

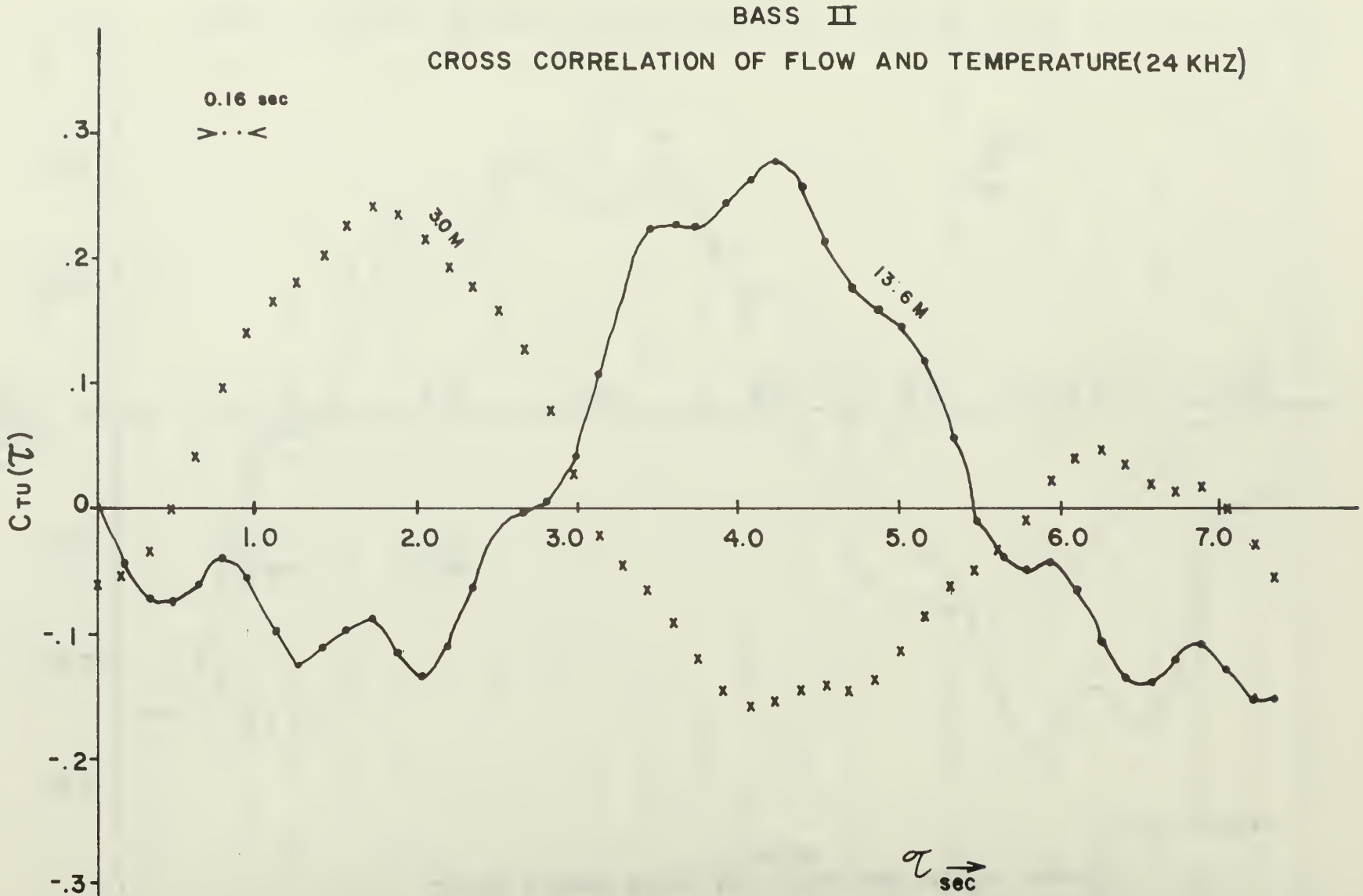

Fig 13. Temporal cross correlation of horizontal flow and temperature fluctuations during 24.4 kHz study at depths 3.0 and 13.7 m. BASS II.

that there is greater variability in the instantaneous total number of bubbles relative to their average number than there is variability in temperature. Tables 2 and 3 show that σ_U / U ranges from about one-third to one-tenth as depth increases. Notice that the near-surface 24.4 kHz correlograms are down to 1/e of their value in about 1 second, whereas the envelope of the temperature-dominated 24.4 kHz correlogram at 13.7 m depth is still above 1/e after as much as 7 seconds' delay. If this reasoning is correct, the spatial correlation function of number of bubbles (if this could be measured) would have a smaller correlation length than the spatial correlation function of excess temperature.

Using the same reasoning as above, we must conclude that the number of resonant bubbles at 95.6 kHz, which determines the character of those correlograms, must be reasonably constant over a 7 second lag time (the maximum calculated). Since the 95.6 kHz bubbles are the smallest ones measured in this experiment, it appears that the small bubbles retain their identity, $\frac{\Delta a}{a} \leq \delta_R/2 \approx .05$, and their gross locations, for a time of at least 7 seconds.

F. Spectra

Data processing of the spectra of ϕ, T and v* have been done with different time lags and different resolutions and band width in order to clarify the spectral implications already deduced from the correlation functions. The previously described "fine structure" that is so prominent in the temperature correlations (Figure 9) and elsewhere, turns out to be an harmonic series with 0.5 Hz fundamental and strong, even, harmonics particularly at

*To avoid confusion with the symbol, u, used for volume fraction, we will use v for the horizontal material velocity in the direction of the sound beam.

1, 2, and 4 Hz. These components are strongest in the material velocity and temperature spectra, and we believe that they represent motion of the equipment frame. Since this oscillating motion is in the presence of much larger D.C. velocities (e.g., $v = 0.64$ m/sec and $\sigma_v = 0.064$ m/sec in one case - see Appendix 3) the even harmonics are emphasized. Further, since the oscillating motion of the frame takes the temperature sensors to positions of different temperature (due to the vertical temperature gradient), the temperatures show similar spectra. In the cases where temperature effects, rather than bubble effects, dominate the fine structure is evident also in the sound phase fluctuations. Since the fine structure is an artifact that is characteristic of our mounting structure rather than the ocean, we will not discuss this aspect of the spectra any further.

A higher resolution ($F^* = 0.025$ Hz), smaller bandwidth ($F_{max} = 0.6$ Hz), presentation of the horizontal velocity component of material velocity at five depths is shown in Figure 14. Previous study[19] has shown that the spectral components of the material velocity in the ocean are well correlated with, and representative of, the ocean surface height spectrum, attenuated and filtered by the depth dependent factor $\exp(-Kz)$, where K is the wave number of the spectral component of the orbital velocity. The velocity spectra of Figure 14, do, indeed, resemble those of an ocean surface height spectrum (confirmed also in Figure 12 of the BASS II Trials Officer's Report[22]) with peak power spectral density (PSD) at the frequency 0.175 Hz.

The behavior of the PSD of $\Phi_v(F)$ at the peak frequency (0.175 Hz) has

*To avoid confusion, we will use the upper case "F" for modulation frequency and the lower case "f" for sound carrier frequency.

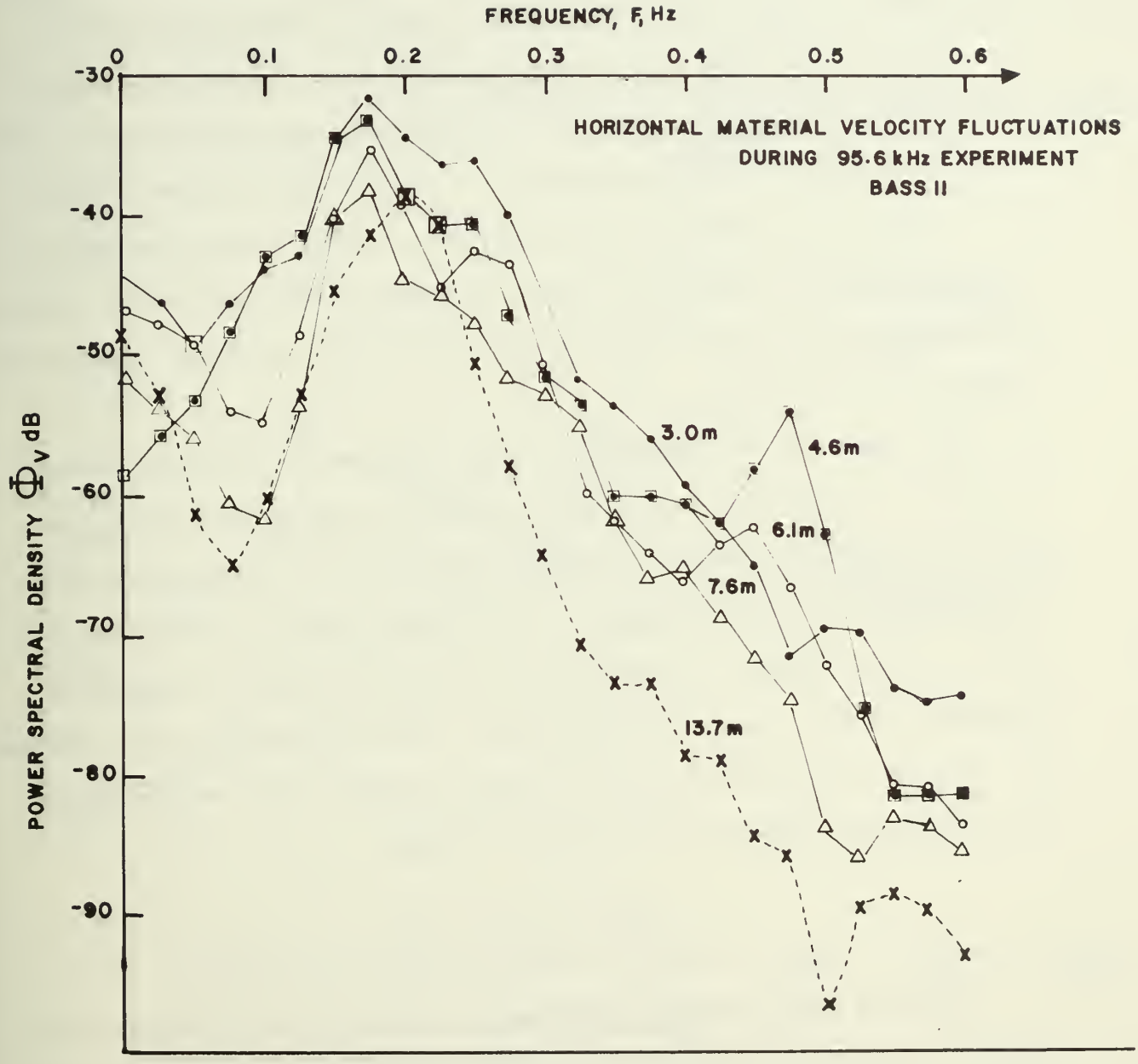

Fig 14. Power spectral densities of fluctuations in the horizontal material velocity at 3.0, 4.6, 6.1, 7.6 and 13.7 m during the 95.6 kHz sound phase study. BASS II.

been identified and replotted in Figure 15 as a function of depth in order to compare with theory. At this frequency, the surface wave number is $K = 0.116\ m^{-1}$. If the spectral component is following the attenuation law with depth, $20\ \log_{10}$ of $\exp(-Kz)$ gives a change of level, with depth of 1.01 dB/m. A best line of this slope has been drawn through the five data points available, and it is seen to quite well represent the behavior of the observed material velocity component. We conclude that the peak component of the underwater particle velocity spectrum in BASS II was principally due to the surface wave height spectrum. The point at which the higher frequency components of the velocity spectrum are dominated by turbulent (non-orbital) components is not clear.

The spectra of the temperature fluctuations at five depths during the 95.6 kHz run are plotted in Figure 16. Since the temperature spectrum involves the manner in which a spatially distributed temperature microstructure is convected past the sensor by the complex motion of the medium with respect to the sensor, the spectrum is much more difficult to comprehend than the velocity spectrum. Nevertheless, some understanding can be deduced. For example, the spectra are due to rates of change of the temperature and are, therefore, measured by the material change,

$$\frac{dT}{dt} = \frac{\partial T}{\partial t} + (\vec{v} \cdot \nabla)T$$

The local rate of change, $\partial/\partial t$, can be assumed to be negligible compared to the convective change if the Taylor Hypothesis of frozen convected scalars is accepted. Since vertical temperature gradients are more likely than horizontal ones, the convective change will be maximum in the z direction, that is, the term $w\ \partial T/\partial z$. Unfortunately, only one electromagnetic

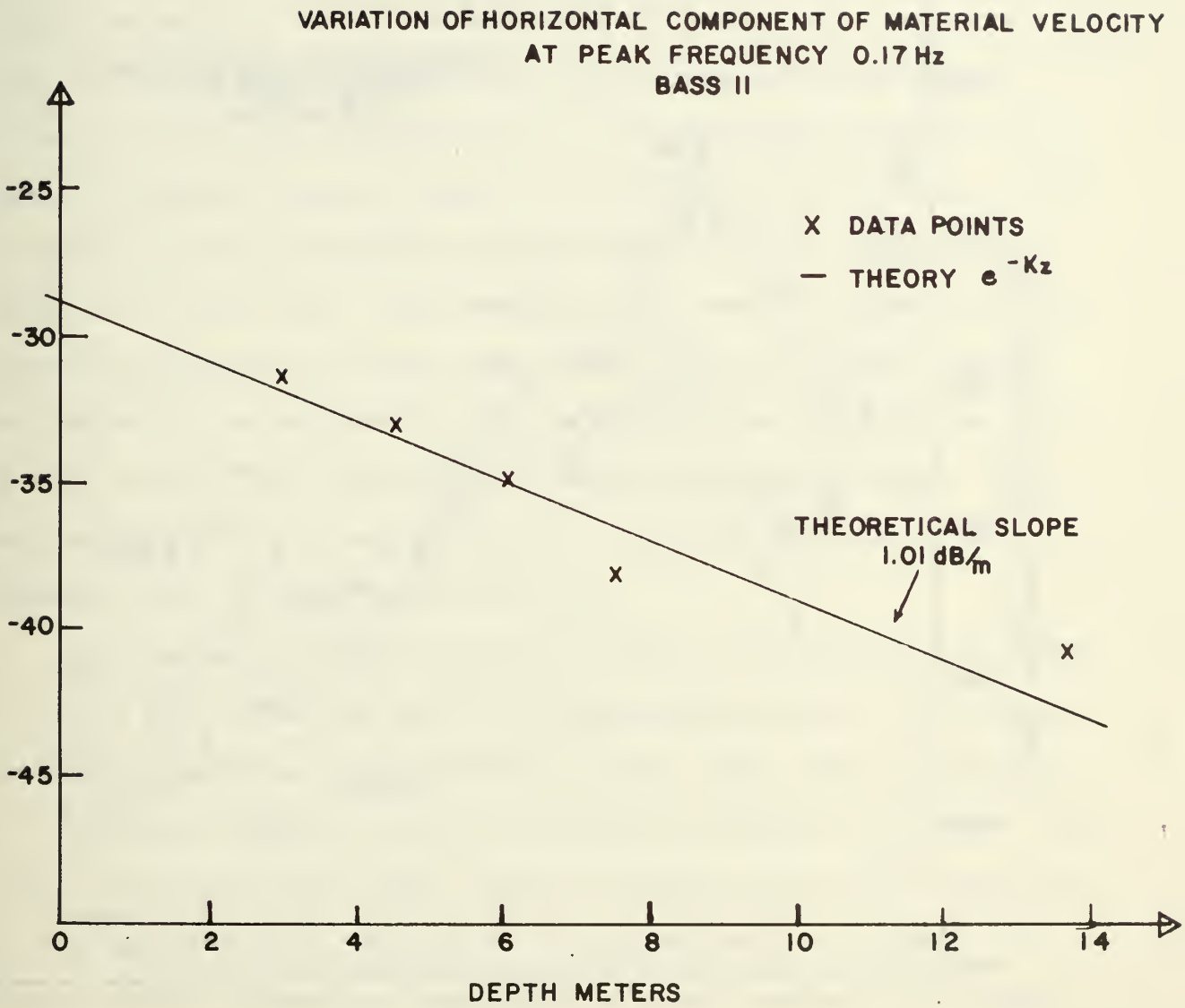

Fig 15. Power spectral densities of horizontal component of material velocity fluctuations at the peak frequency of 0.17 Hz, "x", plotted as a function of depth, and compared with the theoretical attenuation for orbital velocities of surface waves, exp(-Kz) = 1.01 dB/m. BASS II.

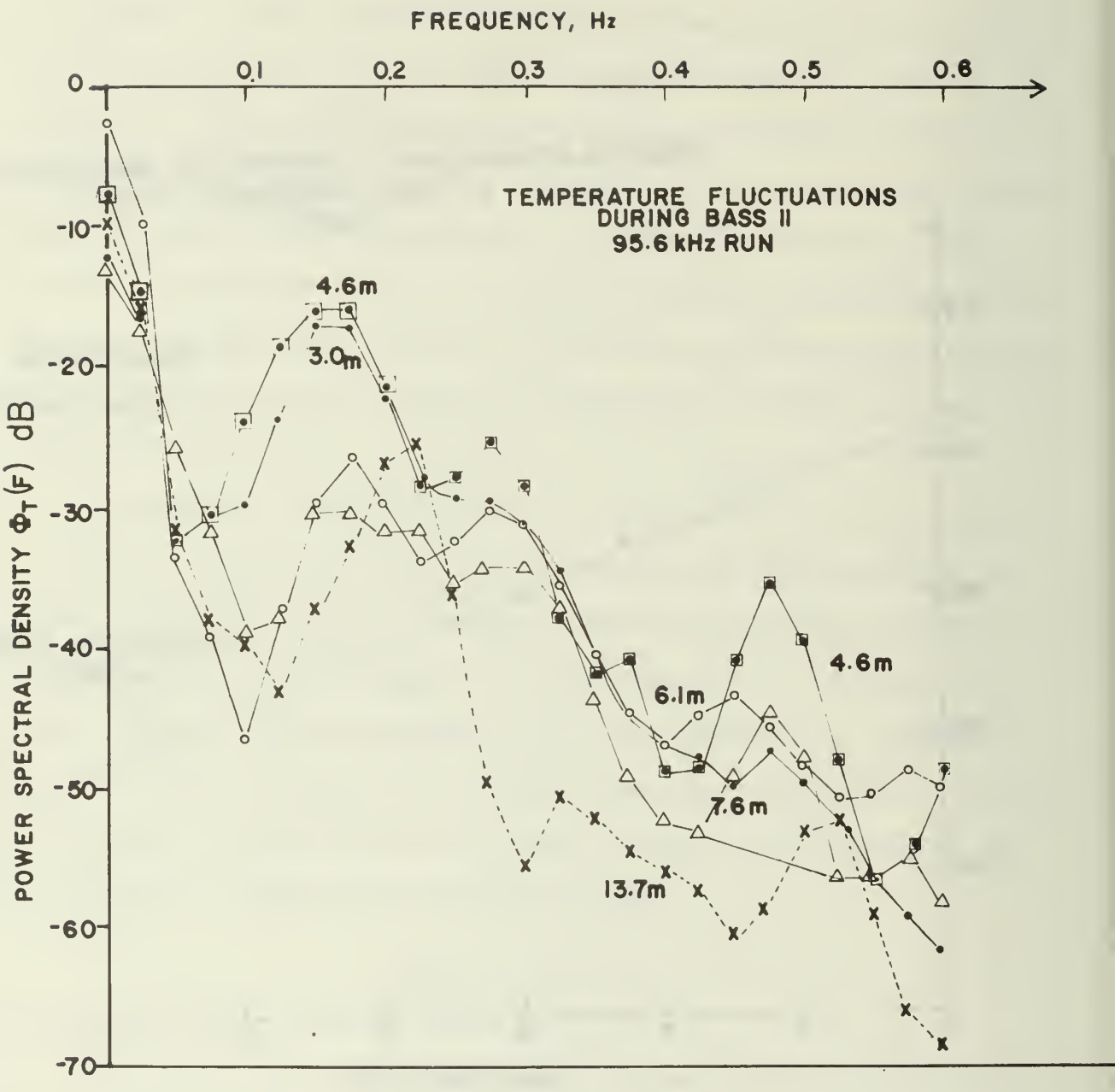

Fig 16. Power spectral densities of fluctuations of temperature at depths 3.0, 4.6, 6.1, 7.6 and 13.7 m. Measurements made during 95.6 kHz sound phase study. BASS II.

flowmeter was available and it was set to measure the horizontal components rather than the vertical. However, our previous discussion of Figure 14 suggests that the component at 0.17 Hz was at the peak of both the pressure and the velocity spectrum, and, therefore, that the z component of the orbital velocity, w, would also peak at this frequency. Now consider Figure 16. We see that even though the vertical component of the material velocity is greater at 3.0 than at 4.6 m, the temperature fluctuation spectrum at the peak frequency is less at the shallower position. This can only be due to a vertical temperature microstructure that has a large gradient $\partial T/\partial z$ at the lower level. This reversal of the expected decrease in Φ_T with increasing depth does not occur at any other level, at the peak frequency. An inversion at approximately 5 m in the BT at 1010 and a "twitch" at about 4 m in the BT at 1415 (see Appendix 2) support our observation that the microstructure at 4.6 m was distinctive. The effect also shows in the $\overline{\sigma_T}$ column of Table 3, during the 95.6 kHz run.

Another feature of the temperature spectra is that the prominent peaks of energy at 0.17 and 0.27 Hz at the shallower depths appear to be shifting to higher frequencies as the depth is increased. This effect appears also in the velocity spectra, and may be evidence of underwater turbulence, uncorrelated with the surface height, which is becoming increasingly significant as the depth increases. If this is the true explanation, it appears that the turbulence spectrum has energy peaks at higher frequencies than those of the orbital velocity spectrum. There is some confirmation of this speculation in the greater than expected value of the velocity at 13.6 m in Figure 15. The temperature spectrum appears to imitate these peaks in the velocity spectrum and therefore to be behaving somewhat like the passive

convected scalar of Batchelor's theory[20].

Spectra of the fluctuations of sound phase are shown in Figures 17, 18, and 19. Compared to 95.6 kHz, the spectra for sound frequency 24.4 kHz are generally flatter and closer to a Gaussian form, as would be expected from the near-Gaussian correlation functions (figures 17, 19). The broader spectra for 24.4 kHz are undoubtedly a consequence of the strong dependence of the sound speed on the bubble fraction, U, which is likely to be Gaussian distributed (statistically) and to have a Gaussian spatial correlation function. We have already pointed out the broad PDF implied by $0.12 \leq \frac{\sigma_U}{U} \leq 0.30$. There is essentially no evidence of the peak surface wave frequency (0.17 Hz) in the 24.4 kHz spectra.

The predominant feature of the phase fluctuations for 95.6 kHz is the strong peak at the ocean surface wave peak frequency of 0.17 Hz*. Figures 18 and 19 show this peak to be common to all depths and to generally decrease in magnitude with increasing depth; this provides additional evidence of our explanation that the fluctuations at this frequency are predominantly due to change of radius caused by the surface wave pressure. Away from this dominant frequency, the spectra at depths 3.0, 6.1, 7.6 and 13.7 m are almost indistinguishable. Beyond F = 0.3 Hz, the 95.6 kHz spectrum at depth 4.6 m shows larger PSDs than at 3.0 m (as does the phase spectrum for frequency 24.4 kHz); this is apparently due to the larger temperature fluctuations at 4.6 m previously observed in Figure 16. Except for this anomaly at 4.6 m,

*For these graphs the resolution is 0.05 Hz so that what was formerly identified as a peak at 0.175 Hz, now is found at 0.15 rather than 0.20 Hz; in all cases we have compromised and arbitrarily assigned the unresolvable value 0.17 Hz to this peak frequency so that we will not cause confusion in the identification by the reader.

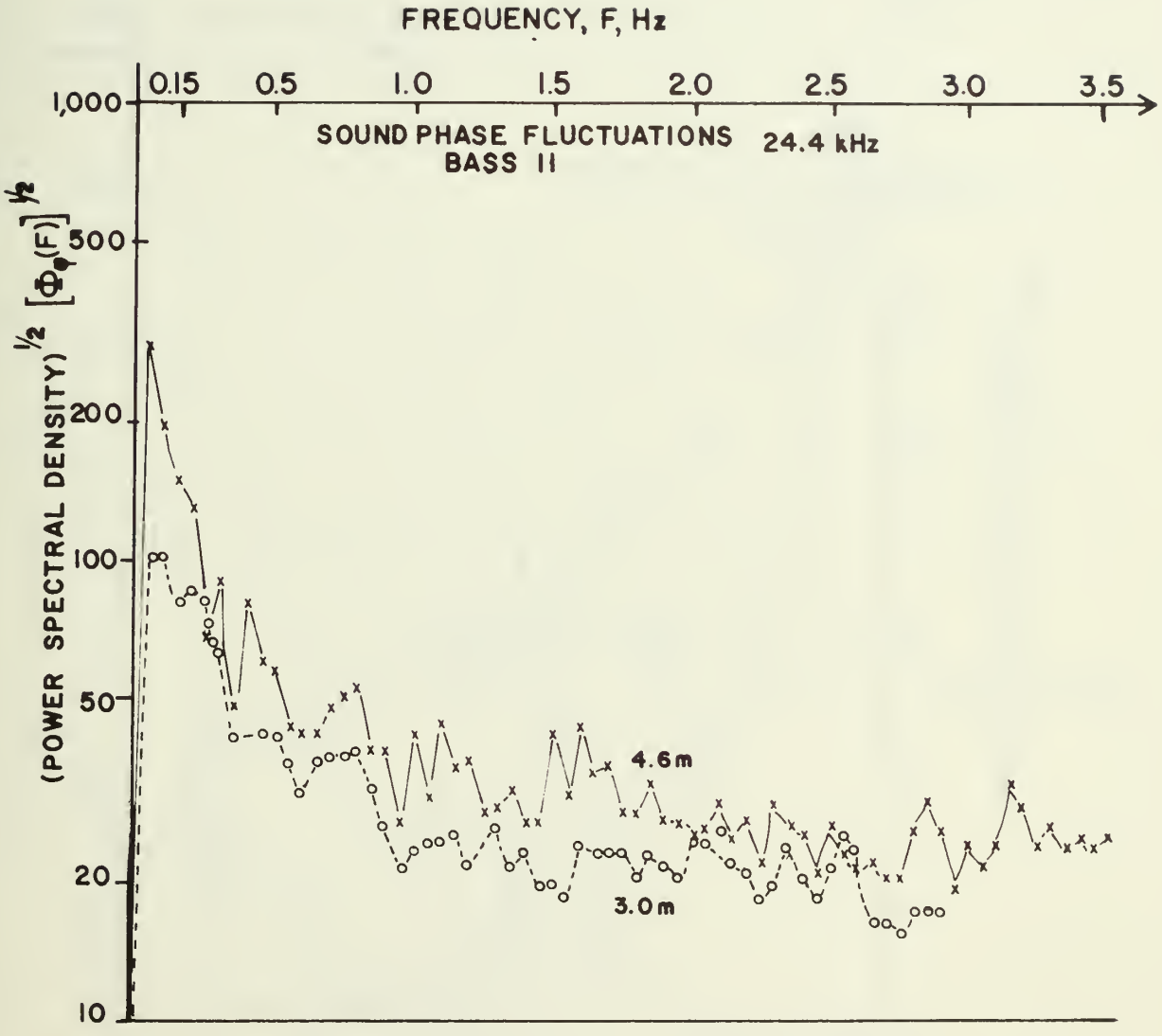

Fig 17. Square root of power spectral densities of 24.4 kHz sound phase fluctuations at depths 3.0 and 4.6 m. BASS II.

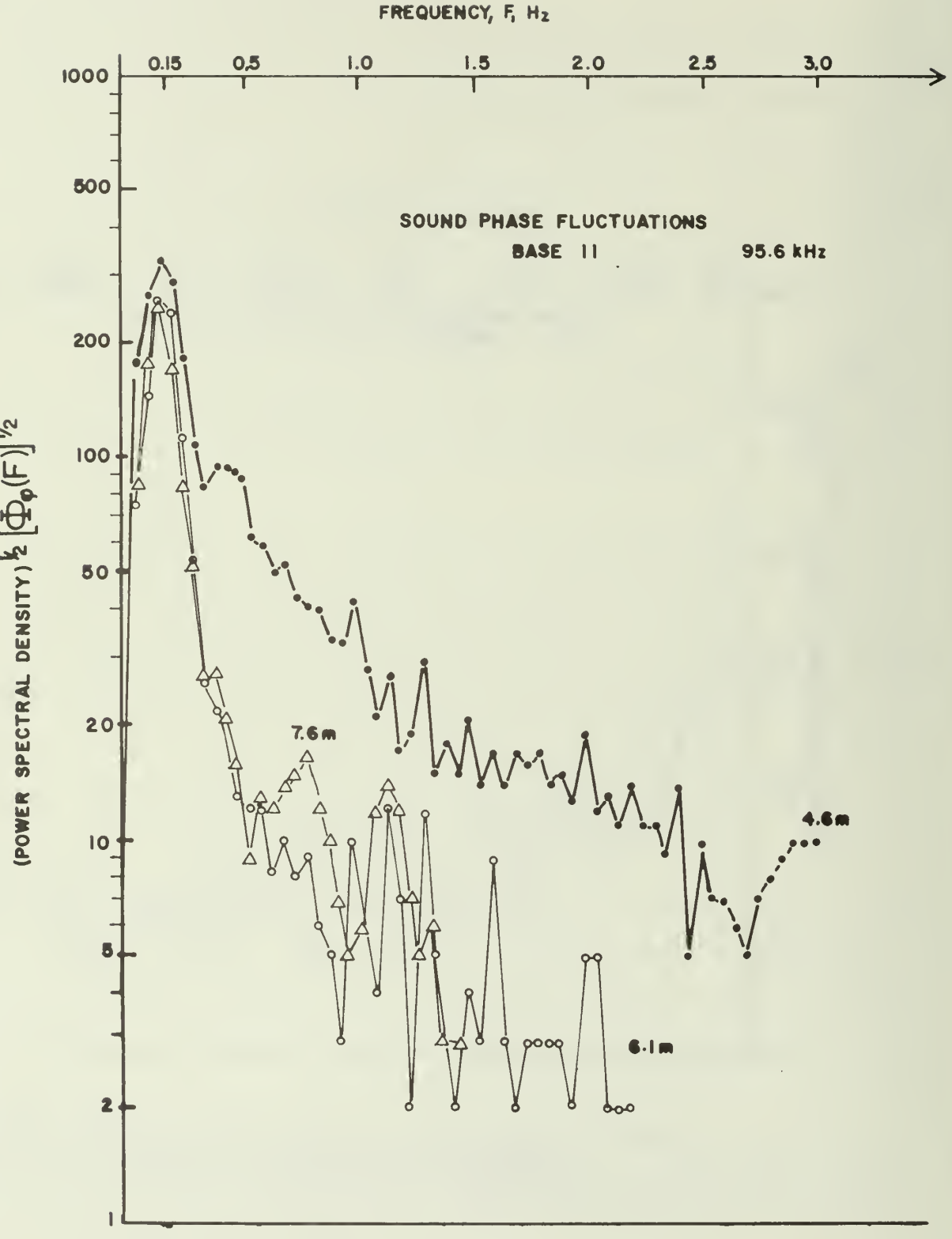

Fig 18. Square root of power spectral densities of 95.6 kHz sound phase fluctuations at depths 4.6, 6.1 and 7.6 m. BASS II.

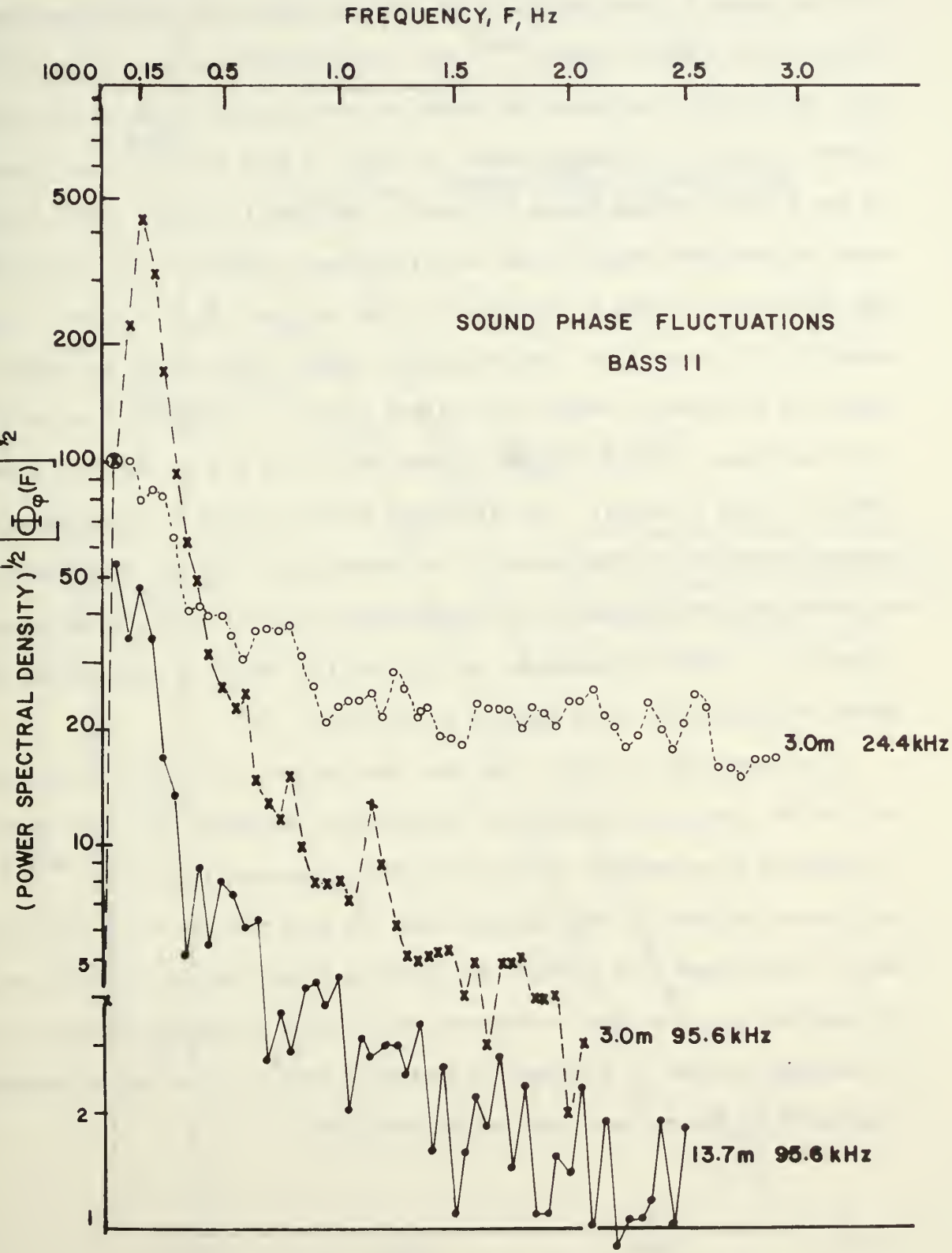

Fig 19. Square root of power spectral densities of 24.4 kHz sound phase fluctuations at 3.0 m and 95.6 kHz sound phase fluctuations at 3.0 and 13.7 m. BASS II.

for $F > 0.17$ Hz, the power spectral density of the phase fluctuations for 95.6 kHz sound follows precisely the F^{-5} law that would be expected for a surface wave pressure effect[21,22] for a fully-developed sea. This is shown most dramatically in Figure 20, where we have replotted some of the data of Figures 18 and 19 on log-log paper in order to show the power law dependence. At low frequencies the phase fluctuation spectrum is almost a twin to the ocean surface wave spectrum and the fifth power law for $F > F_m$ is found at all depths for a range of frequencies from just past $F_m = 0.17$ Hz to approximately $F = 0.5$ or 0.7 Hz. The exception, again, is the case for depth 4.6 m where the fluctuating temperature effect begins to take over from the pressure dependence for $F > 0.35$ Hz (graphs for 4.6 m, 6.1 m, and 13.7 m not shown to avoid crowding). The displaced lines of slope F^{-5} have been replotted versus depth (not shown). The variation of the spectral level with depth has been determined to be approximately exp(-H/4.7 m), which compares fairly well with a determination of (n/a)da from decay of attenuation with depth (reference 10), that behaved as exp(-H/6.7 m).

As a conclusive check to show that the spectrum of phase fluctuations at 95.6 kHz was not determined by the particle velocity, the phase shift due to spectrum of underwater material velocity components, $\Phi(F) = Ae^{-\omega^2 Z/g} F^{-5}$, was plotted separately and compared with the data for the 3.0 m spectrum of phase fluctuations (not shown); the velocity theory did not fit the data. We conclude that the phase modulation at 95.6 kHz is due to changes of radius of resonant bubbles in response to pressures caused by the major frequency components of the surface wave height spectrum.

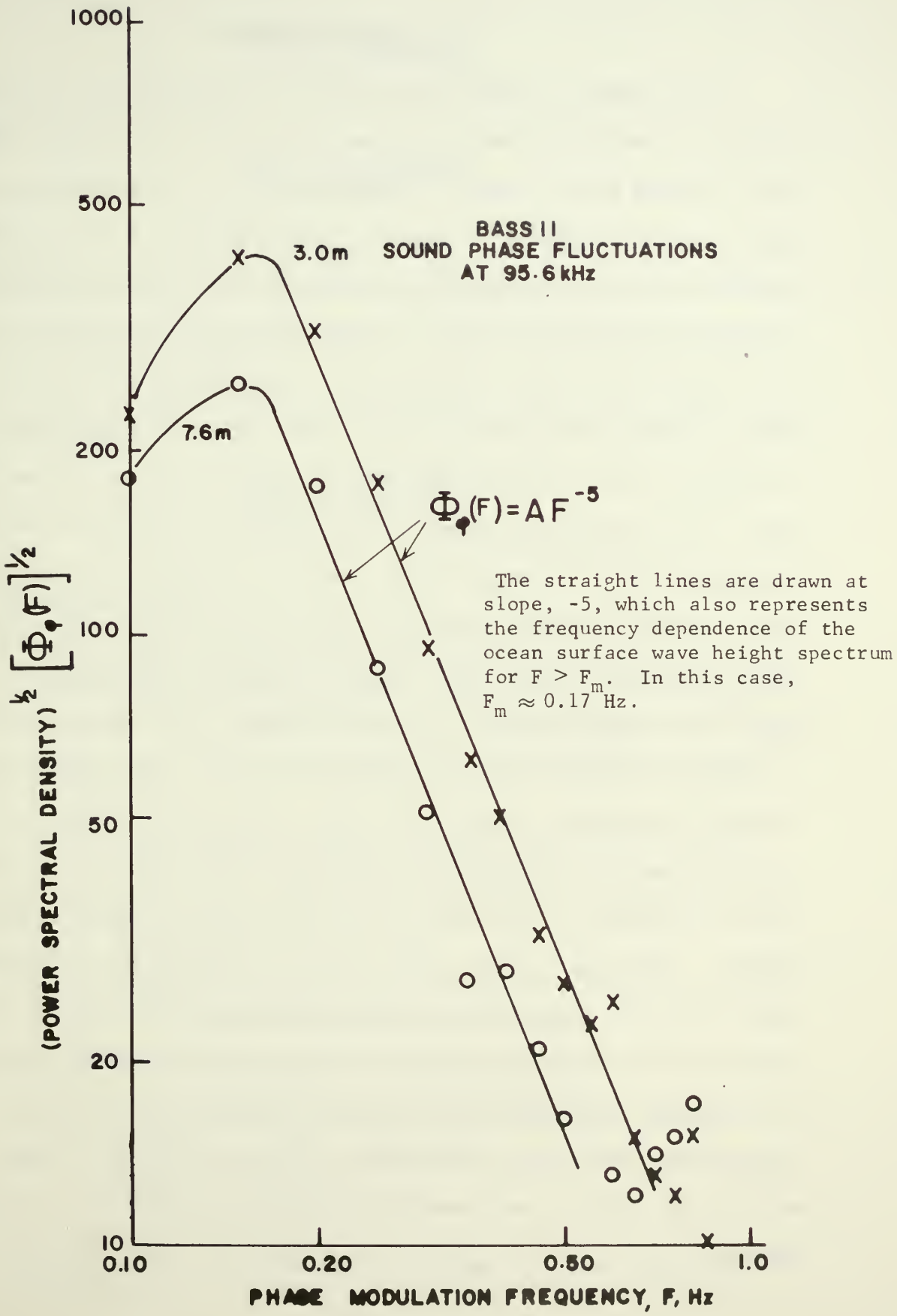

Fig 20. Square root of power spectral densities of 95.6 kHz sound phase fluctuations. BASS II.

VII. ACKNOWLEDGEMENTS

A large number of people made substantial contributions to the conduct and data processing of the experiments described in this report. All data were collected by LCDR James R. Fitzgerald, USN, who volunteered to participate in Project BASS upon completion of his studies at the Naval Postgraduate School, and until ordered to other duty. Mr. Pat Pitt, Applied Research Laboratory, University of Texas, on temporary duty with the Royal Australian Naval Research Laboratory, generously took over the large task of A/D conversion and digital data processing after LCDR Fitzgerald's departure, and did an admirable job of pulling together loose ends and completing the computer work. Direct technician support was provided by Mr. William E. Smith (Naval Postgraduate School) during BASS I, and Mr. S. O'Brien (Royal Australian Naval Research Laboratory, BASS II. The analysis could not have been completed without the large amount of experienced and highly competent computer assistance contributed by Mr. Ian Hagen (RANRL). The entire project received the complete cooperation and generous assistance of all the RANRL personnel involved, including Dr. William F. Hunter, Superintendent; Dr. I. S. F. Jones, Project Leader; Dr. J. H. Ranicar, Assistant Project Leader and Assistant Trials Officers, Mr. J. C. Waller, Mr. E. Kaye, Mr. J. Huggett, and Mr. J. Hibbert. CAPT Jack C. Smith, USN, was the Trials Officer and Project Coordinator who kept the operation running smoothly and who evoked complete assistance from the ESSO/BHP crew which operated our platform, Kingfish A.

Finally, my appreciation to Dean of Research, J. M. Wozencraft (Naval Postgraduate School) and to personnel of Naval Ship Systems Command (PMS 302) who saw the value in, and provided the financial support for, this unusual project.

VIII. APPENDICES

APPENDIX 1

BASS I EXPERIMENTS

I. Data

1. Fluctuations experiment at separations 1.047, 2.045, 4.046 m
2. Decorrelation rate: data at 15, 25, 35 ft depth. One separation. 62.15 kHz.
3. Bubble sweep: data at 28 frequencies from 15 to 97 kHz, 15 ft depth.

BASE II EXPERIMENTS

I. Data

A. Acoustical data

1. Frequency run: four minute runs from 10 kHz; single wavelength differences from 50 to 75 kHz, selected frequencies elsewhere. Depths: 10, 70 (max), 20, 10 ft. Estimated Duration of Recording (EDR): 4 hours; Estimated Duration of Experiment (EDE): 6 hours.
2. Depth run: 10 minute runs at two frequencies, at six depths.
   a. Set frequency at 25 kHz*, vary depth 10, 15, 20, 25, 50, and 70 feet.
   b. Set frequency at 95 kHz, vary depth 70, 50, 25, 20, 15, and 10 feet; EDR: 2 hours; EDE: 3 hours
3. Diurnal run: sound speed as function of time
   a. Set depth 10 feet below trough. Consecutive 10 min runs at 25 kHz* and 65 kHz; repeat every hour for 24 hours. EDR: 8 hours; EDE 24 hours

*Frequency 25 kHz is frequency for which S/N is at least 35 dB

4. Wind run: sound speed during changing wind conditions

   a. Set depth 10 feet below trough. Do continual recording at 25 kHz* during rapidly changing wind conditions.
   EDR: 3 hours; EDE: 3 hours.

5. Range run; sound speed as a function of range; frequencies 25* and 95 kHz at four ranges (10 min runs) at depth 10 feet, then repeat at 70 feet.
   EDR: 3 hours; EDE: 4 hours

B. Auxiliary data needed during all NPS experiments

1. Two horizontal components of flow velocity (u and v); temperature, T; velocimeter fluctuations and frequency averages.

C. Hourly observations needed during NPS experiments

1. XBT from tower

2. Meteorological observations: wind direction, speed, sky coverage, precipitation (height of anemometer)

3. Oceanographic observations: sea state and swell height, and periodicity and direction, white caps, foam.

II. Data Processing

A. Time series graphs to determine validity of recordings

B. Mean values of all data

C. Variance wrt mean value (= zero) for all data

D. Temporal Correlations: corrected c, all data of depth run (6 depths, 2 frequencies) and six-10 min extracts of wind run v, T: one depth run and six-10 min extracts of wind

E. Auto spectra: corrected c at 10 and 70 feet; at 25* and 95 kHz plus 6 winds, u,v,T: at 10 and 70 feet plus u^T, only for 6 winds

F. Cross Spectra, Coherences and Phase Angles: for same data as in F.

NOTES: Speed of sound, c, referred to above, is always speed of sound corrected for phase shift due to longitudinal velocity, u.

APPENDIX 2

BATHYTHERMOGRAMS

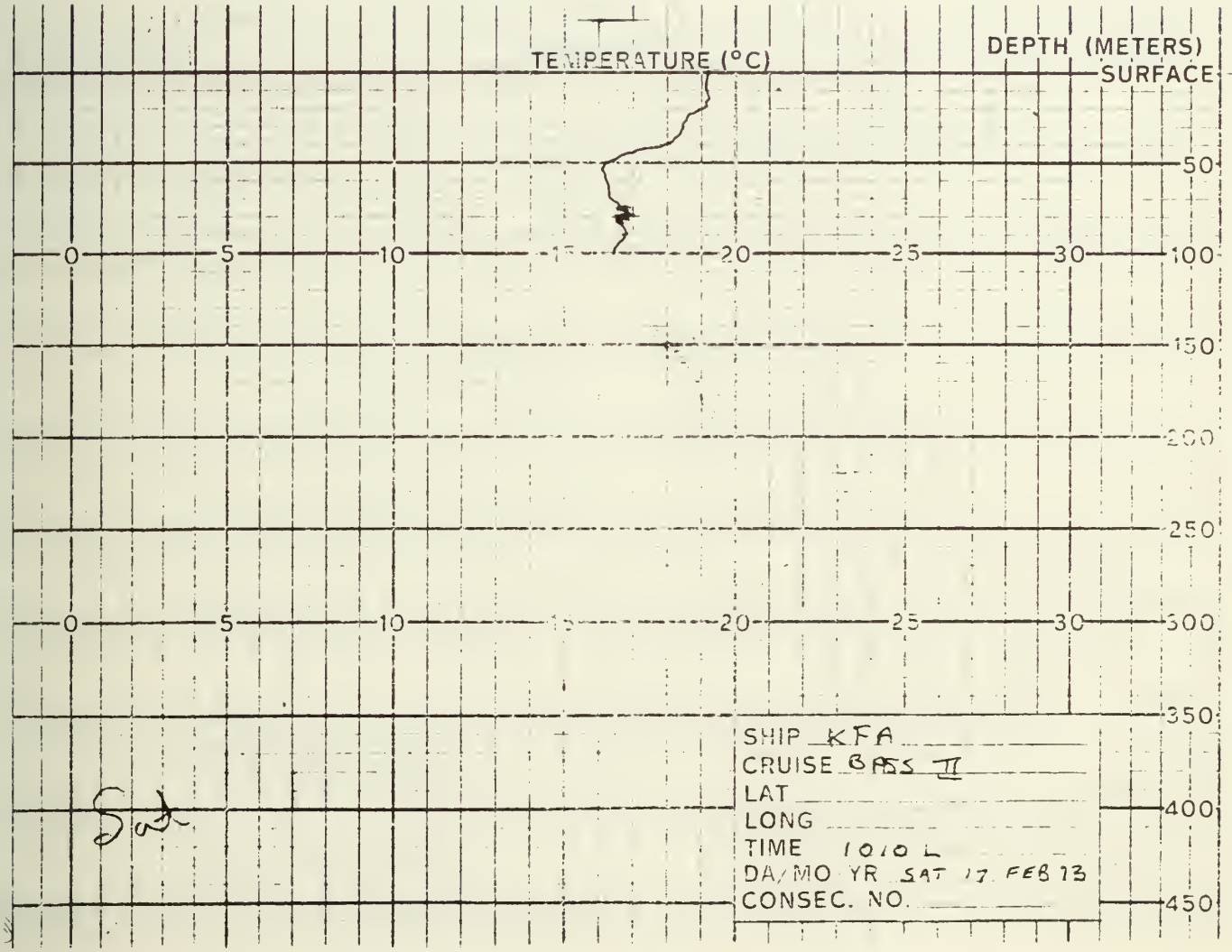

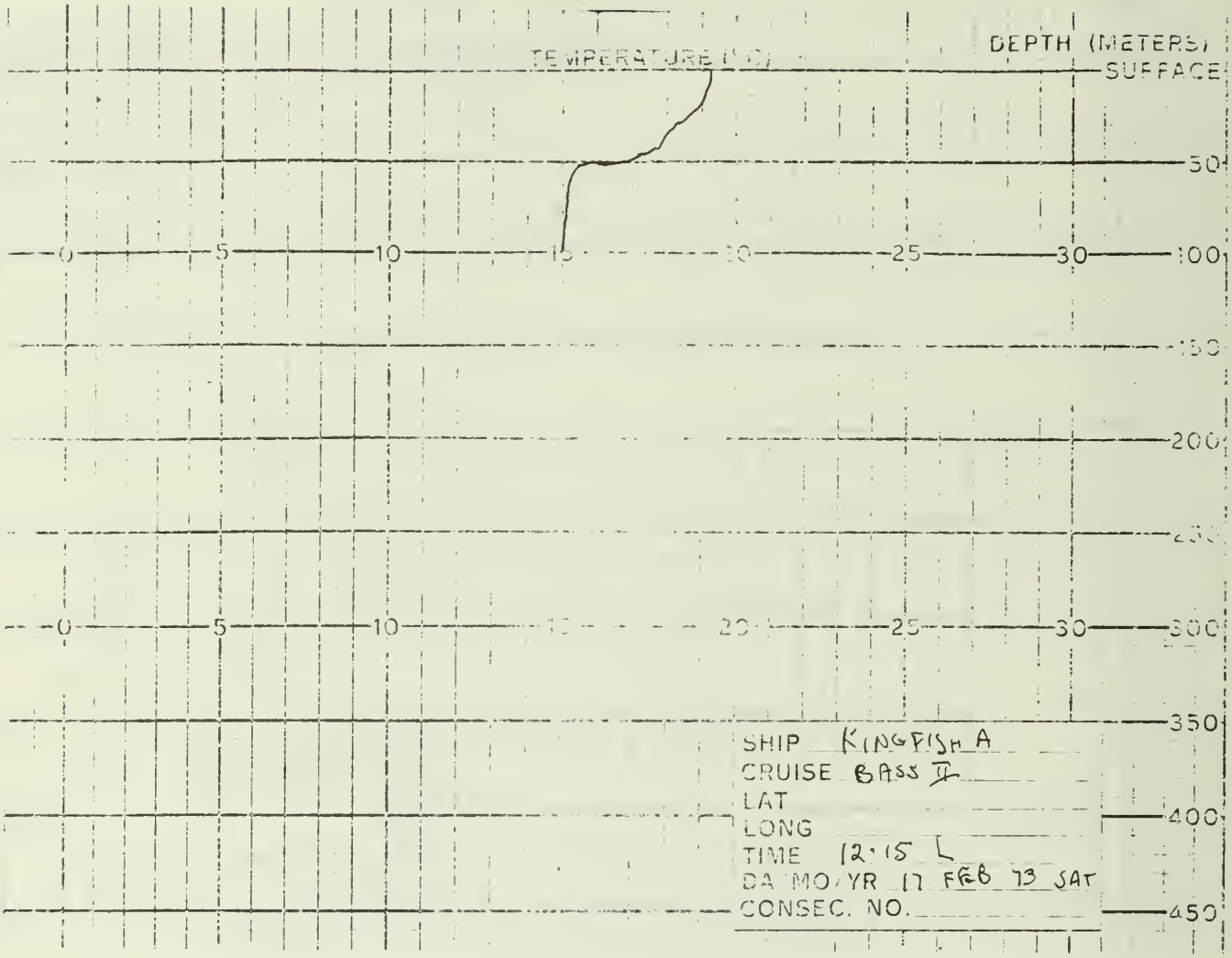
TEMPERATURE (°C)
DEPTH (METERS)
SURFACE
30
100
200
300
350
400
450
0
5
10
15
20
25
30
SHIP KINGFISH A
CRUISE BASS II
LAT
LONG
TIME 12:15 L
DA MO/YR 17 FEB 73 SAT
CONSEC. NO.

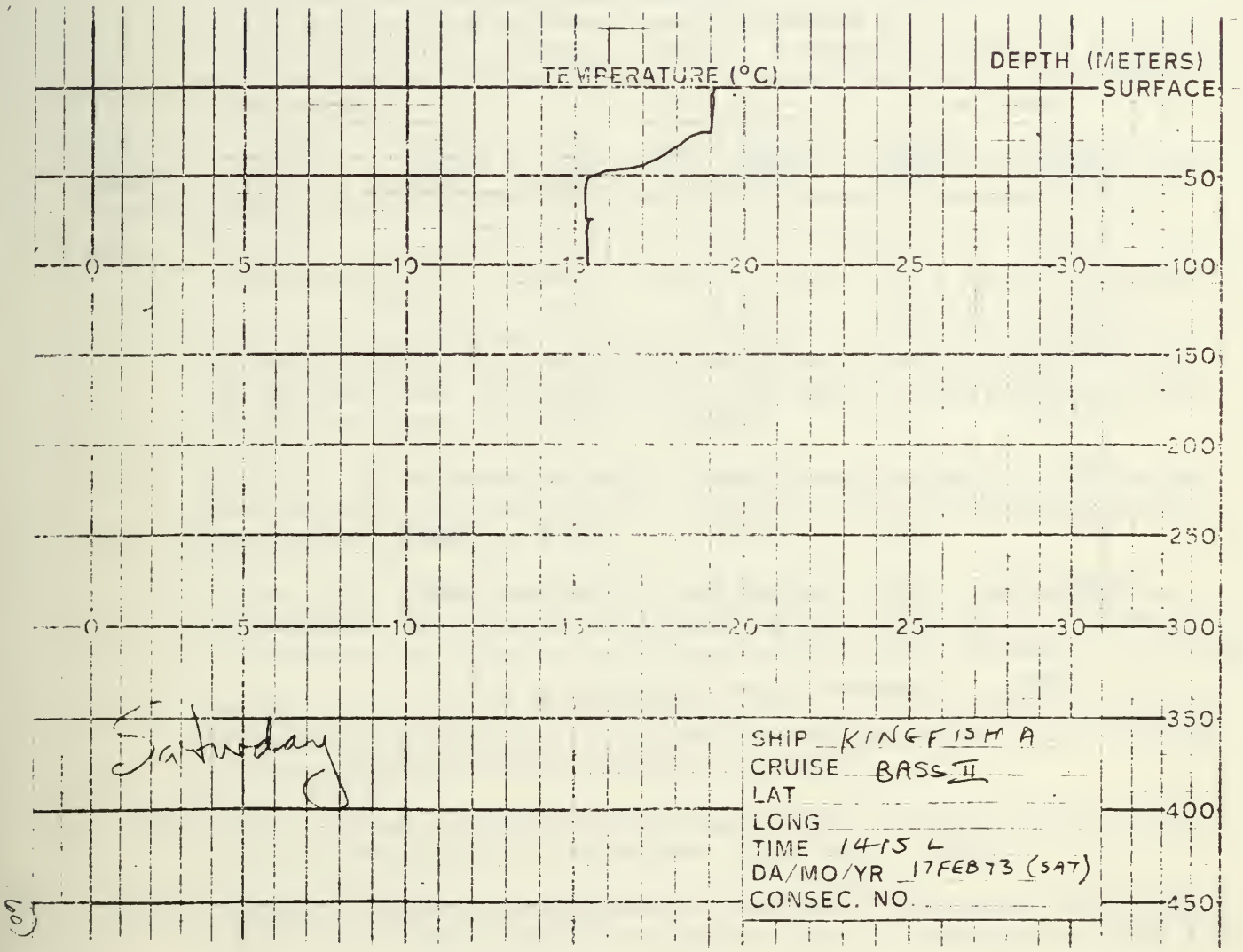
TEMPERATURE (°C)
DEPTH (METERS)
SURFACE
50
100
150
200
250
300
350
400
450
0
5
10
15
20
25
30
0
5
10
15
20
25
30
Saturday
SHIP KINGFISHER
CRUISE BASS II
LAT
LONG
TIME 1415 L
DA/MO/YR 17FEB73 (SAT)
CONSEC. NO.

APPENDIX 3

MATERIAL VELOCITIES CALCULATED FROM ELECTROMAGNETIC FLOWMETER OUTPUT DURING BASS II - 17 FEB 1973

u = horizontal speed in direction of sound path

v = horizontal speed perpendicular to sound path

Clock Time	Depth m	Concurrent sound freq. kHz	$\langle u \rangle$ m/sec	σ_u m/sec	$\langle v \rangle$ m/sec	σ_v m/sec
1110	3.0	24.4	0.23	0.15	0.33	0.18
1235	13.7	24.4	0.64	0.064	–	–
1258	13.7	95.6	0.64	0.071	–	–
1318	7.6	95.6	0.61	0.08	–	–
1343	6.1	95.6	0.56	0.09	–	–
1401	4.6	95.6	0.51	0.10	–	–
1430	3.0	95.6	0.53	0.11	–	–

NOTE: v component output failed after 1130.

IX. REFERENCES

1. Meyer, E. and E. Skudrzyk, Sound Absorption and Sound Absorbers in Water, NAVSHIPS 900.164, Vol 1, 1 Dec 1950.

2. Eckart, C., (Ed) Principles of Underwater Sound, Div. 6, Vol 7, Nat. Def. Res. Coun. Sum Tech Rep., Washington, D. C., 1945.

3. Devin, Charles, Jr., Survey of Thermal, Radiation and Viscous Damping of Pulsating Air Bubbles in Water, J. Acoust. Soc. Amer., 31, 1654-1667, (1959).

4. Blanchard, D. C. and A. H. Woodcock, Bubble Formation and Modification in the Sea and its Meteorological significance, Tellus, 9, 145-158, (1957).

5. Liebermann, L., Air Bubbles in Water, J. App. Phys., 28, 205-211,(1957).

6. Glotov, V. P., Kolobaev, P. A., and Neuimin, G. G., Investigation of the Scattering of Sound by Bubbles Generated by an Artificial Wind in the Sea Water and the Statistical Distribution of Bubble Sizes, Soviet Physics-Acoustics, 7, 341-345, (1962).

7. McCartney, B. S. and B. M. Barry, Echosounding on Probable Gas Bubbles from the Bottom of Saanich Inlet, British Columbia, Deep Sea Research, 12, 285-294, (1965).

8. Zimdar, R. E., Barnhouse, P. D., and Stoffel, M. J., Instrumentation to Determine the Presence and Acoustic Effect of Microbubbles Near the Sea Surface, M.S. Thesis, Naval Postgraduate School, Monterey, CA, (1964).

9. Buxcey, S., McNeil, J. E., and Marks, R. H., Jr., Acoustic Detection of Microbubbles and Particulate Matter Near the Sea Surface.,M. S. Thesis, Naval Postgraduate School, Monterey, CA (1965).

10. Medwin, Herman, In-Situ Acoustic Measurements of Bubble Populations in Coastal Ocean Waters. J. Geoph. Res, 75, 599-611, (1970).

11. Rautmann, Juergen, Sound Dispersion and Phase Fluctuations in the Upper Ocean. M. S. Thesis, Naval Postgraduate School, Monterey, CA, (Dec 1971).

12. Garretson, G , Bubble Transport Theory with Applications to the Upper Ocean. J. Fluid Mech 59, 187-206 (1973).

13. Wang, P.C.C.and H. Medwin, Statistical Considerations to Experiments on the Scattering of Sound by Bubbles in the Upper Ocean. Naval Postgraduate School, Monterey, CA., Tech. Rpt NPS 53Wg72101A, 31 Oct 1972.

14. Figzgerald, James, Statistical Study of Sound Speed in the Inhomogeneous Upper Ocean. M.S. Thesis, Naval Postgraduate School, Monterey, CA, Dec 1972.

15. Medwin, H., The Rough Surface and Bubble Effect on Sound Propagation in Surface Ducts. Naval Postgraduate School, Monterey, CA, Tech Rpt NPS61Md71101A dtd 12 Oct 1971.

16. Chernov, L. A., Wave Propagation in a Random Medium. Dover Publications, New York, 1967.

17. Alexander, C. H., Sound Phase and Amplitude Fluctuations in an Anisotropic Medium. M. S. Thesis, Naval Postgraduate School, Monterey, CA, Dec 1972.

18. Medwin, H. and C. S. Clay, Dependence of Spatial and Temporal Correlation of Forward-scattered Underwater Sound on the Surface Statistics, II, Experiment, J. Acoust. Soc. Amer., 47, 1419-1429, (1970).

19. Bordy, M. W., Spectral Measurement of Water Particle Velocities Under Waves. M. S. Thesis, Naval Postgraduate School, Monterey, CA., 1972.

20. Batchelor, G. K., The Theory of Homogeneous Turbulence. Cambridge Univ. Press, 1953.

21. Phillips, O. M., The Dynamics of the Upper Ocean. Cambridge Univ. Press, 1966.

22. Smith, J. R., RANRL Trials Officer's Report No 1/73, March 1973, Operation BASS II, 5-26 Feb 1973. RANRL, Garden Island, 2000 Australia.

23. Medwin, H., C. S. Clay, J. M. Berkson and D. L. Jaggard, Traveling Correlation Function of the Heights of Wind-blown Water Waves. J. Geoph. Res, 75, 4519-4524, (1970).

INITIAL DISTRIBUTION LIST

	No. Copies
Office of Chief of Naval Operations (OP 964) Attn: Mr. A. S. Rhodes Ballston Tower No. 2 Arlington, Virginia 22203	1
Office of the Director of Defense Research and Engineering Information Office Library Branch The Pentagon Washington, D. C. 20301	1
Defense Documentation Center Cameron Station Alexandria, Virginia 22314	12
Director, Advanced Research Projects Agency Technical Library The Pentagon Washington, D. C. 20301	1
Naval Academy Technical Library Annapolis, Maryland 21401	1
Naval Academy Attn: Prof. L. Crum Annapolis, Maryland 21401	1
Naval Air Systems Command Research and Technology Department of the Navy Washington, D. C. 20360	1
Commanding Officer Naval Air Development Center Johnsville, Warminster, PA, 18974	1
Naval Air Development Center Technical Library Warminster, Pennsylvania, 18974	1
Naval Coastal Systems Laboratory Code P761, Attn: Mr. C. M. Bennett Panama City, Florida 32401	1
Naval Electronics Laboratory Center Library San Diego, California 92152	1

Naval Electronics Systems Command
Research & Technology Directorate
Department of the Navy
Washington, D. C. 20360 — 1

Commanding Officer
Navy Mine Defense Laboratory
Panama City, Florida 32402 — 1

Commander, Naval Oceanographic Office
Attn: Code 1640 (Library)
Washington, D. C. 20390 — 1

Naval Oceanographic Office
Attn: Dr. Morris Schulkin , Associate Director
Washington, D. C. 20390 — 1

Naval Ordnance Systems Command
Research & Technology Directorate
Department of the Navy
Washington, D. C. 20360 — 1

Naval Ordnance Systems Command, NORD 035
Attn: Mr. O. Seidman
Room 6E08, National Center #2
Arlington, Virginia 20360 — 1

Commander, Naval Ordnance Laboratory
Acoustics Division
White Oak, Silver Spring, Maryland 20910 — 1

Naval Ordnance Station
Technical Library
Indian Head, Maryland 20640 — 1

Bureau of Naval Personnel
Department of the Navy
Technical Library
Washington, D. C. 20370 — 1

Naval Postgraduate School
Dean of Research Administration
Code 023
Monterey, California 93940 — 1

Naval Postgraduate School
Chairman, Dept of Physics and Chemistry
Monterey, California 93940 — 1

Naval Postgraduate School
Library - Code 0212
Monterey, California 93940 — 1

Naval Postgraduate School
Department of Mathematics
Code 53Wg , Prof. P.C.C.Wang
Monterey, California 93940 — 1

Naval Postgraduate School
Dept of Physics and Chemistry
Dr. H. Medwin, Code 61Md
Monterey, California 93940 — 5

Director, Naval Research Laboratory
Library, Code 2029 (ONRL)
Washington, D. C. 20390 — 2

Director, Naval Research Laboratory
Technical Information Division
Washington, D. C. 20390 — 2

Director, Naval Research Laboratory
Electronics Division, Code 5267
Attn: Mr. Walton Bishop
Washington, D. C. 20390 — 1

Naval Research Laboratory
Underwater Sound Reference Div.
Technical Library
P. O. Box 8337
Orlando, Florida 32806 — 1

Naval Research Laboratory
Dr. P. Wilkniss, Code 8330
Washington, D. C. 20390 — 1

Commander, Naval Ship Systems Command
Attn: Code PMS 302-4
Department of the Navy
Washington, D. C. 20360 — 2

Commander, Naval Ship Systems Command
Attn: Code PMS 388
Department of the Navy
Washington, D. C. 20360 — 1

Commander, Naval Ship Systems Command
Sonar Directorate (Ships 901)
Department of the Navy
Washington, D. C. 20360 — 1

Commander, Naval Ship Systems Command
RDT&E Planning Division
Department of the Navy
Washington, D. C. 20360 — 1

Naval Ships Systems Command 1
Ships 0311
Attn: Miss B. S. Orleans
National Center No. 3
Arlington, Virginia 20360

Naval Ship Engineering Center 1
Philadelphia Div. Technical Library
Philadelphia, PA 19112

Naval Ship Research & Development Center 1
Central Library
Washington, D. C. 20034

Naval Ship Research & Development Center 1
Attn: Dr. Murrary Strasberg
Washington, D. C. 20007

Naval Ship Research & Development Center 1
E. M. Stanley, Code A 723.2
Annapolis Laboratory
Annapolis, Maryland 21402

Naval Ship Research & Development Center 1
Dr. J. Dickey
Annapolis Laboratory
Annapolis, Maryland 21402

Commander, Navy Undersea Center 1
Technical Library
San Diego, California 92152

Commander, Naval Undersea Center 1
Attn: Dr. Peter Barakos
San Diego, California 92132

Commander, Naval Undersea Center 1
Attn: Dr. A. G. Fabula
San Diego, California 92132

Commanding Officer, Naval Underwater Systems Command 1
Technical Library
Fort Trumbull, New London, Conn 06321

Commanding Officer, Naval Underwater Systems Command 1
Attn: Dr. Robert Mellen
Fort Trumbull, New London, Conn 06321

Commanding Officer, Naval Underwater Systems Command 1
Technical Library
Newport, Rhode Island 02840

Naval Weapons Center 1
Technical Library
China Lake, California 93555

Office of Naval Research (Code 468) 2
800 N. Quincy Street
Arlington, Virginia 22217

Office of Naval Research (Code 461) 1
800 N. Quincy Street
Arlington, Virginia 22217

Office of Naval Research (Code 480) 1
800 Quincy Street
Arlington, Virginia 22217

Office of Naval Research 1
Statistics and Probability Program
Attn: Dr. B. J. McDonald
800 Quincy Street
Arlington, Virginia 22217

Dr. J. B. Hersey 1
Office of Naval Research (Code 102-OS)
Department of the Navy
Washington, D. C. 20360

Office of Naval Research 1
San Francisco Area Office
50 Fell Street
San Francisco, California 94102

Dr. W. F. Hunter, Superintendent 1
Royal Australian Naval Research Laboratory
Garden Island
New South Wales, Australia 2000

Dr. I. Jones 1
Royal Australian Naval Research Laboratory
Garden Island
New South Wales, Australia 2000

Mr. P. Pitt 1
Royal Australian Naval Research Laboratory
Garden Island
New South Wales, Australia 2000

Research Director, NOAA 1
National Ocean Data Center
Rockville, Maryland 20852

Dr. Larry P. Atkinson, Research Associate 1
Skidaway Institute of Oceanography
University System of Georgia
55 West Bluff Road
Savannah, Georgia 31406

Dr. Duncan C. Blanchard, ES 322 1
State University of New York at Albany
1400 Washington Avenue
Albany, New York 12203

Dr. Richard Clarke 1
Theoretical Studies
SACLANT ASW Research Centre
APO New York 09019

Prof. C. S. Clay 1
Dept. of Geology & Geophysics
Geophysical & Polar Research Center
University of Wisconsin, 6118 University Ave.
Middleton, Wisconsin 53562

Dr. Paul A. Crowther 1
Naval Division
Marconi
Chobham Road
Frimley, Camberly, Surrey
England

Dr. Ira Dyer 1
Chairman, Dept of Ocean Engineering
Massachusetts Institute of Technology
Cambridge, Massachusetts 02139

Dr. B. S. McCartney 1
National Institute of Oceanography
Wormley, Godalming Surrey
England

M. Henri Mermoz 1
Laboratoire de Detection Sous-Marin
Le Brusc (Var), France

Dr. Eric Risness 1
Admiralty Underwater Weapons Establishment
Portland, Dorset
England

Dr. John C. Scott 1
University of Essex
Fluid Mechanics Research Institute
Wivenhoe Park
Colchester CO4 3SQ
England

Dr. V. G. Welsby 1
Dept of Electronic & Electrical Engineering
The University of Birmingham
P. O. Box 363
Birmingham 15, England

Dr. David Weston 1
Admiralty Research Laboratory
Teddington, Middlesex
England

Mississippi Test Facility 1
Earth Resources Lab, Code GA
Attn: Mr. Sidney L. Whitley
Bay St. Louis, Mississippi 39520

Librarian 1
Applied Research Laboratory
University of Texas
Austin, Texas 78712

Ordnance Research Laboratory 1
Librarian
Box 30
State College, PA 16801

Unclassified

Security Classification

DOCUMENT CONTROL DATA - R & D

(Security classification of title, body of abstract and indexing annotation must be entered when the overall report is classified)

1. ORIGINATING ACTIVITY *(Corporate author)*

Naval Postgraduate School
Monterey, California 93940

2a. REPORT SECURITY CLASSIFICATION

Unclassified

2b. GROUP

3. REPORT TITLE

Sound Speed Dispersion and Fluctuations in the Upper Ocean: Project BASS

4. DESCRIPTIVE NOTES *(Type of report and inclusive dates)*

Technical Report, NPS-61Md73101A,

5. AUTHOR(S) *(First name, middle initial, last name)*

Herman Medwin

6. REPORT DATE	7a. TOTAL NO. OF PAGES	7b. NO. OF REFS
31 October 1973	73	14

8a. CONTRACT OR GRANT NO.

b. PROJECT NO.

c.

d.

9a. ORIGINATOR'S REPORT NUMBER(S)

NPS 61Md73101A

9b. OTHER REPORT NO(S) *(Any other numbers that may be assigned this report)* To be issued also by RAN Research Laboratory, Garden Island 2000, Sydney, Australia

10. DISTRIBUTION STATEMENT

Approved for public release; distribution unlimited.

11. SUPPLEMENTARY NOTES

Research support: U.S.Naval Ship Systems Command, Code 302, and Royal Australian Naval Research Laboratory.

12. SPONSORING MILITARY ACTIVITY

Naval Postgraduate School
Monterey, California 93940

13. ABSTRACT

Simultaneous measurements of ocean microstructure and sound phase shift from a stable platform in BASS STRAIT, AUSTRALIA, have provided new relations between the statistics of the medium and the statistics of the local sound phase speed near the sea surface in the open ocean. Because of dispersion due to ambient bubbles, average phase speeds in the frequency range 15 to 100 kHz differ as much as 2.5 m/sec from the accepted 3 MHz "precision" velocimeter values down to depths of 7.6 m in the presence of wind speeds of 25-30 knots. These differential speeds imply average bubble volume fractions of the order of 10^{-7} with standard deviations approximately one-fifth of the mean value. The differential sound speed is now shown to increase approximately proportional to the wind speed. The third power decrease of differential speed with increasing depth is roughly verified. Under these experimental conditions the predominant cause of the local phase fluctuations at 24.4 and 95.6 kHz is shown to be bubble activity rather than temperature fluctuations. At 24.4 kHz the activity is the random change of number of bubbles. At a frequency such as 95.6 kHz, where there is a large resonant bubble population, the predominant part of the frequency spectrum of the sound phase modulation is shown to be caused by changing bubble radius due to the fluctuating ocean surface wave height. The sound phase spectrum mimics the wind wave spectrum given by Pierson and Moskovitz to two octaves beyond the frequency of the peak energy, at which point the surface pressure effect has dropped low enough for temperature fluctuations to take over. A theory is presented for prediction of these microstructural sound phase fluctuations from a knowledge of the surface wave height spectrum.

DD FORM 1 NOV 65 1473 (PAGE 1)

S/N 0101-807-6811

Unclassified

Security Classification

A-31408

14 KEY WORDS	LINK A		LINK B		LINK C	
	ROLE	WT	ROLE	WT	ROLE	WT
Sound Fluctuations						
Speed of Sound						
Ocean Bubbles						

147254
QC233
.M43 Medwin
Sound speed dispersion
and fluctuations in the
upper ocean.